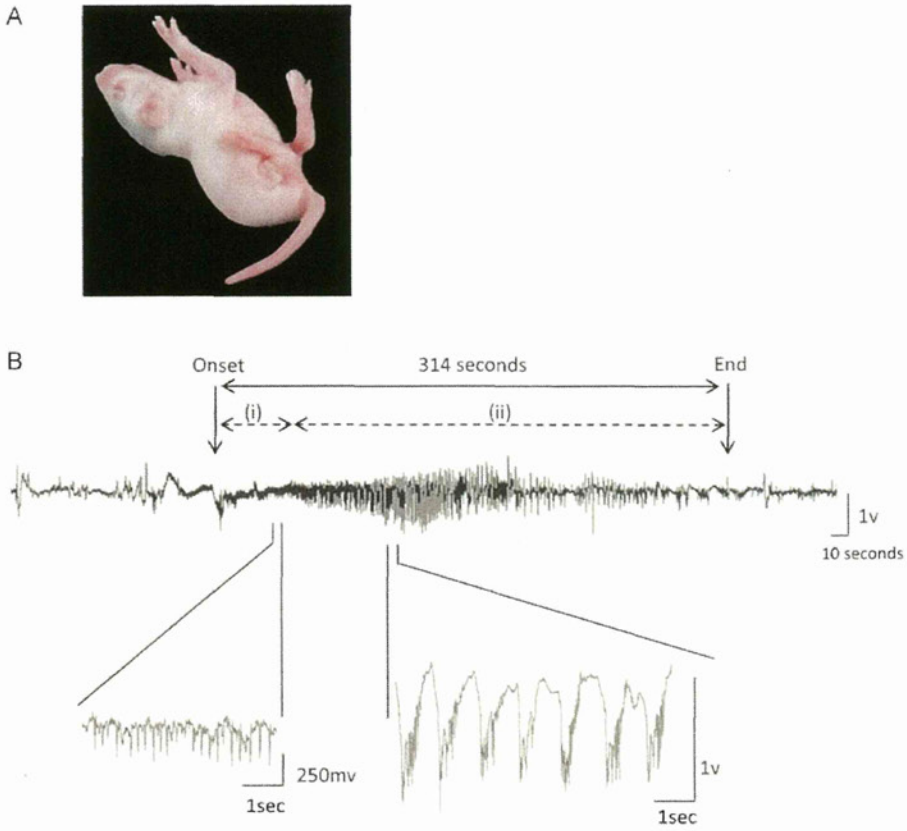

Figure 5. Spontaneous epileptic seizures in homozygous $Lgi1^{L385R/L385R}$ rats. (**A**) Photography during a spontaneous seizure in a P10 $Lgi1^{L385R/L385R}$ rat showing asymmetric clonie of the four limbs. (**B**) Epidural EEG recording in a P10 $Lgi1^{L385R/L385R}$ rat showing the onset and the end of an electroclinical seizure (trace corresponds to left cortex). Behavioral modifications are correlated with EEG event; (i) tonic attack and (ii) jerking.

Effect of antiepileptic drugs on audiogenic seizures

Finally, we evaluated the efficacy of several antiepileptic drugs on audiogenic seizures in primed $Lgi1^{+/+}$ and $Lgi1^{+/L385R}$ rats. We administered carbamazepine, phenytoin, levetiracetam or ethosuximide intraperitoneally (20 mg/kg) 30 min before the auditory stimuli in 8-week-old rats (Table 1, Supplementary Material, Movie S3). Both wild running and GTCS were completely inhibited by carbamazepine and phenytoin in $Lgi1^{+/+}$ and $Lgi1^{+/L385R}$ rats. Levetiracetam prevented wild running and GTCS in three of four $Lgi1^{+/L385R}$ rats. No ictal EEG activity was detected during auditory stimulation (not shown). Ethosuximide, a prototypic generalized absence seizure drug, had no effect on seizures of $Lgi1^{+/L385R}$ rats ($n = 4$).

DISCUSSION

Here, we present the first genetically engineered animal model expressing a missense mutation in the *Lgi1* gene as found in patients with ADLTE. We generated and characterized an *Lgi1*-mutant rat with the L385R mutation and studied its functional consequences *in vivo*. We first examined the impact of the mutation using an *in vitro* overexpression paradigm. Our results showed that this mutation prevented Lgi1 secretion in transiently transfected COS7 cells, indicating that it apparently shares common effects with ADLTE-causing missense mutations which nearly all, except one, decrease protein secretion (31). Testing endogenous expression levels of the mutated Lgi1 protein in cultured cortical neurons of *Lgi1*-mutant animals revealed very low levels of L385R-Lgi1 protein, both in extracellular medium from cultures and also in neuron lysates. Moreover, endogenous levels of Lgi1 protein were also substantially lower in the brain of *Lgi1*-mutant rats than of WT littermates. Probably, *in vivo*, the L385R mutation favors misfolding and so reduces Lgi1 protein stability, causing its degradation through protein quality-control mechanisms. This is consistent with *in silico* models predicting that a number of missense disease-causing mutations alter protein folding (31). Thus, a physiopathological loss of function may emerge not only due to a failure of protein secretion as suggested by *in vitro* experiments but also from a lack of correctly folded neuronal Lgi1. This new mechanism must be considered together with previous suggestions of a defective secreted extracellular Lgi1 (acting as a ligand for ADAM22/23 at the post-synaptic) (23), rather than cytoplasmic (through the modulation of Kv1.1 channel) (22). In this model, the *Lgi1*-mutant rat carrying a missense mutation located nearby a naturally occurring missense mutation found in ADLTE patients (3,12,14) lacks both cytoplasmic

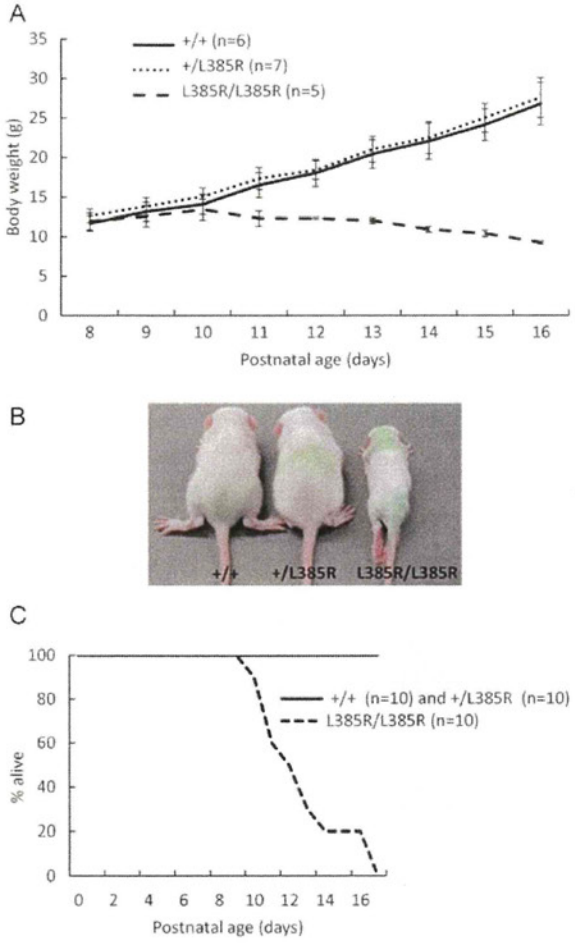

Figure 6. Premature death and reduced body weight in homozygous $Lgi1^{L385R/L385R}$ rats. (**A**) Body weight was comparable for $Lgi1^{+/+}$ ($n = 6$), $Lgi1^{+/L385R}$ ($n = 7$) and $Lgi1^{L385R/L385R}$ ($n = 5$) animals at birth. The body weight of $Lgi1^{L385R/L385R}$ rats became reduced with respect to $Lgi1^{+/L385R}$ and $Lgi1^{+/+}$ rats after P10. (**B**) Photography shows $Lgi1^{L385R/L385R}$ rats smaller than $Lgi1^{+/L385R}$ and $Lgi1^{+/+}$ littermates at P14. (**C**) The Kaplan–Meier survival curves of $Lgi1^{+/+}$ ($n = 10$), $Lgi1^{+/L385R}$ ($n = 10$) and $Lgi1^{L385R/L385R}$ ($n = 10$) rats from P0 to P17. All $Lgi1^{L385R/L385R}$ rats had died at P17.

and extracellular Lgi1. While cortical tissue from patients is not available, we speculate that ADLTE-causing missense mutations might also lead to instability *in vivo*, causing a haploinsufficiency. We note such a deficiency in Lgi1 occurs in patients with limbic encephalitis and seizures, in which the immune-mediated disruption of LGI1 results in hyperexcitability (11).

While focal epilepsies are often associated with brain lesions, we observed no major abnormality in the brain morphology of *Lgi1*-mutant rats, although subtle changes could not be ruled out at this level of analysis. Moreover, we found no obvious defect in neuritic outgrowth or neuronal life-span in cortical cultures from *Lgi1*-mutant rats, contrary to previous reports, suggesting that Lgi1 may promote neurite outgrowth (25,32). We thus conclude that ADLTE pathogenesis due to the L385R mutation in Lgi1 may involve a hyperexcitability due to altered neuronal network activity rather than abnormal dendritic development.

The phenotype of *Lgi1*-mutant rats possessed similarities to the ADLTE syndrome. Epileptic seizures, associated with cortical and hippocampal ictal epileptiform activity, emerged at P10 in homozygous $Lgi1^{L385R/L385R}$ pups. Frequent and severe seizures led to death of the animals around P13. $Lgi1^{+/L385R}$ rats, which carry a heterozygous missense mutation recapitulating the human genetic cause, did not generate seizures spontaneously but were highly susceptible to audiogenic seizures, as patients with *LGI1* mutations (seizures may be triggered by noises or voices) (6). In addition, we showed that rat audiogenic seizures responded to the same drugs as used in the human: they were suppressed by two antiepileptic drugs, carbamazepine and phenytoin, that target voltage-gated channels, but also by levetiracetam which anticonvulsant activity is mediated through interaction with the synaptic vesicle protein 2A (SV2A) (33,34). Since Lgi1 co-immunoprecipitates with several other neuronal vesicle-related proteins (35), this latter pathway involving SV2A might be promising for preventing seizures in this syndrome. As expected, ethosuximide, a first choice drug for absence seizures, did not prevent audiogenic seizures. This rat model thus permitted more detailed studies on audiogenic seizures and tests on antiepileptic molecules. As SV2A, Lgi1 may point toward novel antiepileptic therapies for drug-resistant patients.

The phenotype of *Lgi1*-mutant rats and *Lgi1* knockout mice that we generated (20) were comparable with a clear gene dosage relation between Lgi1 and epileptic syndromes: severe early onset spontaneous seizures without gross brain anatomical abnormalities occurred in homozygous animals, and a high susceptibility to audiogenic seizures in adult heterozygous animals. Spontaneous seizures shared similar features: age at onset (P10), duration and behavioral manifestations consisting of wild running followed by tonic and/or clonic events, ictal epileptic activities present in both the hippocampus and the cortex and seizure severity causing animals to fail to gain weight by P10 and die prematurely a week after seizure onset. We note, however, that spontaneous events were more frequent in *Lgi1*-mutant rats (~8/h) than in $Lgi1^{-/-}$ mice (~1–2/h). In our previous study, we concluded that seizures probably originated in the hippocampus of $Lgi1^{-/-}$ mice since hippocampal ictal activity preceded cortical discharges. Seizures may also be initiated in the hippocampus of *Lgi1*-mutant rats, although we have no direct evidence on this point. We note the striking restricted time window (P10) when seizures emerge in both $Lgi1^{-/-}$ mice and *Lgi1*-mutant rats. The timing of seizure onset was not exactly correlated with that of Lgi1 expression. Lgi1 expression preceded seizure onset both in mice, in which it was detected at E9.5 in the primitive eye (19) or E16 in whole brain lysate (20), and in rats, in which we show an expression as early as P0 in brain lysate (Supplementary Material, Fig. 2S). Most probably, onset of seizures is related to the period of brain developmental changes, common to rats and mice, embracing maturation of excitatory synapses of the cortex and hippocampus and/or the switch in the polarity of GABAergic signaling by inhibitory interneurons (36). This natural history of seizures beginning within the 3 first weeks of life, followed by death shortly after, is common to several epileptic

Table 1. Audiogenic seizures

Genotype	Prime stimulation	Target stimulation	Antiepileptic drugs	Number of rats			
				Total	No seizure	Wild running only	Wild running + GTCS
+/+	−	+	−	11	11	0	0
+/+	+	+	−	14	0	10	4
+/L385R	−	+	−	15	15	0	0
+/L385R	+	+	−	22	0	0	22
+/+	+	+	Carbamazepine	3	3	0	0
+/+	+	+	Phenytoin	2	2	0	0
+/L385R	+	+	Carbamazepine	6	6	0	0
+/L385R	+	+	Phenytoin	4	4	0	0
+/L385R	+	+	Levetiracetam	4	3	1	0
+/L385R	+	+	Ethosuximide	4	0	0	4
+/L385R	+	+	Saline solution	5	0	0	5

Prime stimulation at age P16 was applied as follow: 120 dB, 10 kHz for 5 min. Target stimulation at 8 weeks of age was performed as follow: 120 dB, 10 kHz for 1 min. Antiepileptic drugs (20 mg/kg) were injected intraperitoneally 30 min before auditory stimulation.

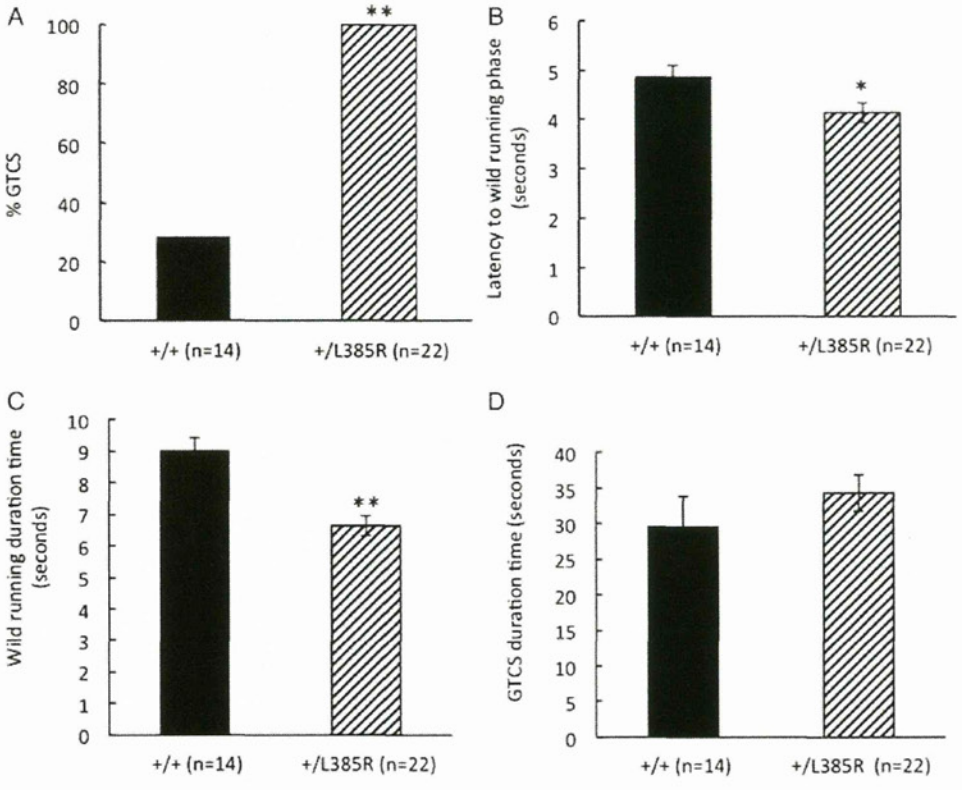

Figure 7. Susceptibility to audiogenic seizures. (**A**) Primed rats were tested at 8 weeks for audiogenic seizures with a stimulus of 10 kHz, 120 dB applied for 1 min. GTCSs were induced in all $Lgi1^{+/L385R}$ rats but in only 28% of $Lgi1^{+/+}$ rats. (**B**) The time to onset of wild running was shorter in $Lgi1^{+/L385R}$ rats than in $Lgi1^{+/+}$ rats. (**C**) The duration of wild running was shorter in $Lgi1^{+/L385R}$ than in $Lgi1^{+/+}$ rats. (**D**) The duration of GTCS was not significantly different between $Lgi1^{+/L385R}$ ($n = 22$) and $Lgi1^{+/+}$ ($n = 4$). $^{**}P < 0.01$ and $^{*}P < 0.05$ by Student's t-test.

mice models, including $ADAM23^{-/-}$ (32), $ADAM22^{-/-}$ (37), $Kv1.1^{-/-}$ (38) and $Scna1^{-/-}$ (39) mice.

In conclusion, we report a unique and original rat model of *Lgi1*-related epilepsies, which is complementary to knockout mice. It gave us the opportunity to better understand the consequences of missense mutations on the fate of the mutant Lgi1 protein, revealing a major finding that L385R-Lgi1 protein is unstable *in vivo*, explaining the severe epileptic phenotype of *Lgi1*-mutant rats. We speculate that the overall similar phenotype observed in homozygous *Lgi1*-mutant rats (L385R-Lgi1) and $Lgi1^{-/-}$ mice (the absence of Lgi1) is due to the rapid degradation of Lgi1-L385R leading to a

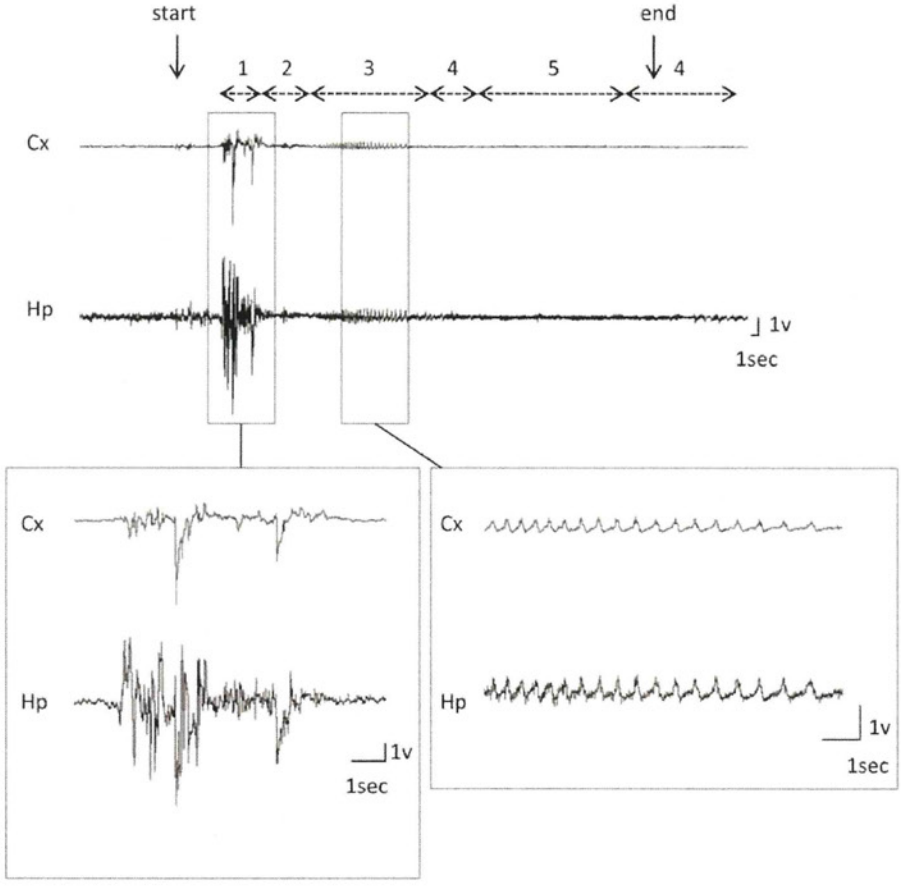

Figure 8. EEG recording in $Lgi1^{+/L385R}$ rat during an audiogenic seizure. Traces of typical cortical and hippocampal EEG responses to auditory stimuli from an 8-week-old $Lgi1^{+/L385R}$ rat. Behavioral changes were correlated with EEG events: 1, wild running; 2, tonic attack; 3, clonic convulsions; 4, immobility; 5, alternative knee bending exercise. Movement artifacts are present on the EEG signal during the wild running phase and mostly suppressed in the second tonic phase. Rhythmic low-voltage slow activities were observed in the third clonic phase, in cortex and hippocampus. They decreased in the fourth immobility phase and were suppressed in the final phase until the end of the stimulus. Cx, cortex; Hp, hippocampus.

haploinsufficiency equivalent to a gene knockout. Thanks to this model, we also investigated the consequences of *Lgi1*-deficiency on the neuronal and neurite outgrowth. Finally, the heterozygous $Lgi1^{+/L385R}$ rats allowed us to initiate pharmacological studies on their sound-induced seizures, which replicate the auditory triggering of seizure in the human.

MATERIALS AND METHODS

ENU mutagenesis in rats

ENU mutagenesis and screening protocols using MuT-POWER in rats have been described (29). The sperm archive KURMA has been deposited in the National BioResource Project-Rat in Japan (NBRP-Rat: www.anim.med.kyoto-u.ac.jp/nbr). Primers were designed to amplify by PCR the exonic region of the rat *Lgi1* gene from ~50 bp flanking each intron (Supplementary Material, Table S1). Sequencing was performed with BigDye terminator mix, followed by the protocol for the Applied Biosystems 3100 DNA Sequencer. *Lgi1*-mutant rats were recovered from frozen sperm by intracytoplasmic sperm injection.

Animals

Lgi1-mutant rats (strain name, F344-$Lgi1^{m1kyo}$) were deposited in NBRP-Rat (N° 0656). They were kept and bred at the Institute of Laboratory of Animals, Graduate School of Medicine, Kyoto University, in air-conditioned rooms under a 14 h light/10 h dark cycle. Animal care and experiments were conformed to the Guidelines for Animal Experiments and were approved by the Animal Research Committee of Kyoto University.

Genotyping of *Lgi1*-mutant rats

Exon 8 of *Lgi1* was amplified by PCR with Ex8-1 primers (Supplementary Material, Table S1) using the Ampdirect Plus® PCR buffer (Shimadzu) and FTA® card for blood samples. PCR products were then sequenced with BigDye terminators mix.

Western blots

Littermate rat P5, P9 and P12 pups were decapitated; whole brains were quickly removed and lysed in 3 M urea, 2.5% dodécylsulfate de sodium, 50 mM Tris, 30 mM NaCl buffer (total brain homogenates). For synaptic fractions, brains of littermate rats were homogenized in 50 mM Tris, 5 mM acide éthylène diamine tétraacétique 120 mM NaCl with complete inhibitor cocktail, spun for 1 h at 165 000 × *g* and pellets resuspended with 1% Triton X-100. Total protein concentrations were determined by the bicinchoninic acid assay method (Pierce). Twenty-five micrograms of each sample was separated on 10% Tris-glycine polyacrylamide gels were analyzed by western blot with the following antibodies: rabbit polyclonal anti-Lgi1 antibody (ab30868; 1 μg/ml; Abcam), goat polyclonal anti-Lgi1 antibody (sc-9583; 1 μg/ml; Santa Cruz) and rabbit anti-actin antibody (1/1000, Sigma Aldrich).

Cell culture and transfection

Drs K. Senechal and J. Noebels kindly provided the mouse WT Lgi1 cDNA with a Flag-tag at the N terminus. Lgi1-E383A and Lgi1-L385R were generated using the Quik-Change® Site-Directed Mutagenesis Kit. COS7 cells were cultured in Dulbecco modified Eagle's minimal essential medium containing 10% fetal bovine serum, penicillin and streptomycin. Transient transfections were performed using Lipofectamine™ 2000 according to instructions (Invitrogen), followed by a 14–16-h incubation in serum-free media. Cells and media were analyzed 24–36 h after transfection. Cell lysates and conditioned media were prepared as described (14) and analyzed by western blot.

Neuronal cultures

Primary cortical and hippocampal cultures were prepared from the brains of 10 individual rat embryos at E19. Neurons were dissociated using the Nerve-Cell culture system and were plated at 10^5 cells/ml in neuron culture medium (Sumitomo Bakelite Co.) on 35-mm poly-L-lysine coated dishes. Each culture was derived from a single embryo. Cultures were daily observed for 21 days. Neuronal outgrowth was imaged and measured automatically using ImageJ.

Quantitative RT–PCR

Whole brains were removed from P9 rats ($Lgi1^{+/+}$, $n = 5$; $Lgi1^{+/L385R}$, $n = 7$; $Lgi1^{L385R/L385R}$, $n = 5$) and stored in RNA-*later*® solution (Applied Biosystems). Total RNA was isolated with RNeasy Miniprep columns (Qiagen) and contaminating DNA was depleted using RNase-free DNase. First-strand cDNA was synthesized from 5 μg of total RNA by oligo dT-primed reverse transcription (*ThermoScript*™ Reverse Transcriptase, Invitrogen). Quantitative PCRs were performed as triplicates using the QuantiFast Multiplex PCR Kit (Qiagen) with predesigned probes for rat *Lgi1* (QuantiFast Probe Assays) and peptidylprolyl isomerase A (PPIA) as a reference gene included in all multiplex PCRs. The error bars of the quantitative PCR represent SDs of triplicates.

Brain histochemistry

$Lgi1^{+/+}$ ($n = 1$), $Lgi1^{+/L385R}$ ($n = 2$) and $Lgi1^{L385R/L385R}$ ($n = 1$) littermates aged P12 were deeply anesthetized with sodium pentobarbital (50 mg/kg by intraperitoneal injection). Brains were removed, fixed in Bouin's fixative and embedded in paraffin. Morphological changes were evaluated from hematoxylin and eosin-stained, 4-μm thick paraffin sections.

Animal surgery and intracranial EEG recordings

Cortical EEG was recorded from $Lgi1^{L385R/L385R}$ P10 rats (during 3 continuous hours) and $Lgi1^{+/+}$ and $Lgi1^{+/L385R}$ rats aged 8 weeks. Rats were anesthetized with an intraperitoneal injection of sodium pentobarbital (40 mg/kg) and the heads were fixed in a stereotaxic instrument. One-mm-diameter screw electrodes were implanted into the epidural space of the left frontal cortex. A reference electrode was fixed on the frontal cranium. For hippocampal EEG, 0.2-mm-diameter stainless-steel electrodes were implanted in the hippocampus (3.8 mm caudal, 2.0 mm lateral to the bregma and 2.2 mm from the cortex surface). A miniature plug was positioned and fixed on the midline of the skull to provide electrical connections. After 1-h recovery period for P10 rats and 1-week recovery period for 8-week-old rats, animals were placed in a shielded box (40 × 40 × 40 cm^3) and the EEG signals were amplified with a sampling rate of 0.5–100 Hz with a 8-channel system (MEG-6108; Nihon Kohden) and recorded (RTA-1100; Nihon Kohden) under free-moving conditions. The signals were stored in a computer for analysis (ML845; PowerLab). Behavioral changes were simultaneously observed with video recording.

Acoustic stimulation

The testing apparatus consisted of a 17 × 25 × 13-cm^3 plastic cage placed inside a larger sound-proof box. Acoustic stimulation was administered from a loudspeaker (JBL Professional) centrally placed on the cover of the cage. Tone bursts were delivered by a sound stimulator (DPS-725, Dia Medical System Co.) and the signal was amplified using a power amplifier (D75-A, Amcron). $Lgi1^{+/L385R}$ and $Lgi1^{+/+}$ littermate rats were exposed individually to intense auditory stimulation after 1-min habituation. Priming stimulation was performed in P16 rats with a sound stimulus of 120 dB at 10 kHz for 5 min. Target stimulation consisted of a 120-dB sound stimulus at 10 kHz for 1 min at 8 weeks (40). The onset, latency and duration of wild running and GTCS were measured from video records.

Antiepileptic drugs administration

Antiepileptic drugs (Sigma-Aldrich) were administrated intraperitoneally 30 min before target stimulation with therapeutic range (20 mg/kg). Carbamazepine and ethosuximide were first dissolved in polyethylene glycol 400 then in water. Phenytoin

was first dissolved in 0.5 N NaOH and then diluted with saline solution. Levetiracetam was dissolved in saline solution.

SUPPLEMENTARY MATERIAL

Supplementary Material is available at *HMG* online.

ACKNOWLEDGEMENTS

We would like to thank Philippe Couarch and Yayoi Kunihiro for technical help, Aurélien Dauphin for imaging, Sophie Rivaux-Pechoux for statistical analysis and Richard Miles, Vincent Navarro and Yukihiro Ohno for helpful discussion.

Conflict of Interest statement. None declared.

FUNDING

This work was supported by Japan Society of the Promotion of Sciences (to S.B. and S.I.); Agence Nationale de la Recherche (ANR-10-JCJC-1407), European FP6 Integrated Project EPICURE; European large-scale functional genomics in the rat for translational research (FP7-EURATRANS; 241504); Ministry of Education, Culture, Sports, Science and Technology Grant-in-Aid for Scientific Research (16200029) and Industrial Technology Research Grant Program in 2008 from New Energy and the Industrial Technology Development Organization of Japan (to T.M.).

REFERENCES

1. Baulac, S. and Baulac, M. (2010) Advances on the genetics of Mendelian idiopathic epilepsies. *Clin. Lab. Med.*, **30**, 911–929.
2. Morante-Redolat, J.M., Gorostidi-Pagola, A., Piquer-Sirerol, S., Saenz, A., Poza, J.J., Galan, J., Gesk, S., Sarafidou, T., Mautner, V.F., Binelli, S. *et al.* (2002) Mutations in the LGI1/Epitempin gene on 10q24 cause autosomal dominant lateral temporal epilepsy. *Hum. Mol. Genet.*, **11**, 1119–1128.
3. Kalachikov, S., Evgrafov, O., Ross, B., Winawer, M., Barker-Cummings, C., Martinelli Boneschi, F., Choi, C., Morozov, P., Das, K., Teplitskaya, E. *et al.* (2002) Mutations in LGI1 cause autosomal-dominant partial epilepsy with auditory features. *Nat. Genet.*, **30**, 335–341.
4. Michelucci, R., Poza, J.J., Sofia, V., de Feo, M.R., Binelli, S., Bisulli, F., Scudellaro, E., Simionati, B., Zimbello, R., D'Orsi, G. *et al.* (2003) Autosomal dominant lateral temporal epilepsy: clinical spectrum, new epitempin mutations, and genetic heterogeneity in seven European families. *Epilepsia*, **44**, 1289–1297.
5. Winawer, M.R., Ottman, R., Hauser, W.A. and Pedley, T.A. (2000) Autosomal dominant partial epilepsy with auditory features: defining the phenotype. *Neurology*, **54**, 2173–2176.
6. Michelucci, R., Pasini, E. and Nobile, C. (2009) Lateral temporal lobe epilepsies: clinical and genetic features. *Epilepsia*, **50**, 52–54.
7. Ho, Y.Y., Ionita-Laza, I. and Ottman, R. (2012) Domain-dependent clustering and genotype-phenotype analysis of LGI1 mutations in ADPEAF. *Neurology*, **78**, 563–568.
8. Nobile, C., Michelucci, R., Andreazza, S., Pasini, E., Tosatto, S.C. and Striano, P. (2009) LGI1 mutations in autosomal dominant and sporadic lateral temporal epilepsy. *Hum. Mutat.*, **30**, 530–536.
9. Lai, M., Huijbers, M.G.M., Lancaster, E., Graus, F., Bataller, L., Balice-Gordon, R., Cowell, J.K. and Dalmau, J. (2010) Investigation of LGI1 as the antigen in limbic encephalitis previously attributed to potassium channels: a case series. *Lancet Neurol.*, **9**, 776–785.
10. Irani, S.R., Alexander, S., Waters, P., Kleopa, K.A., Pettingill, P., Zuliani, L., Peles, E., Buckley, C., Lang, B. and Vincent, A. (2010) Antibodies to Kv1 potassium channel-complex proteins leucine-rich, glioma inactivated 1 protein and contactin-associated protein-2 in limbic encephalitis, Morvan's syndrome and acquired neuromyotonia. *Brain*, **133**, 2734–2748.
11. Lalic, T., Pettingill, P., Vincent, A. and Capogna, M. (2011) Human limbic encephalitis serum enhances hippocampal mossy fiber-CA3 pyramidal cell synaptic transmission. *Epilepsia*, **52**, 121–131.
12. Senechal, K.R., Thaller, C. and Noebels, J.L. (2005) ADPEAF mutations reduce levels of secreted LGI1, a putative tumor suppressor protein linked to epilepsy. *Hum. Mol. Genet.*, **14**, 1613–1620.
13. Striano, P., Busolin, G., Santulli, L., Leonardi, E., Coppola, A., Vitiello, L., Rigon, L., Michelucci, R., Tosatto, S.C.E., Striano, S. *et al.* (2011) Familial temporal lobe epilepsy with psychic auras associated with a novel LGI1 mutation. *Neurology*, **76**, 1173–1176.
14. Chabrol, E., Popescu, C., Gourfinkel-An, I., Trouillard, O., Depienne, C., Senechal, K., Baulac, M., LeGuern, E. and Baulac, S. (2007) Two novel epilepsy-linked mutations leading to a loss of function of LGI1. *Arch. Neurol.*, **64**, 217–222.
15. de Bellescize, J., Boutry, N., Chabrol, E., Andre-Obadia, N., Arzimanoglou, A., Leguern, E., Baulac, S., Calender, A., Ryvlin, P. and Lesca, G. (2009) A novel three base-pair LGI1 deletion leading to loss of function in a family with autosomal dominant lateral temporal epilepsy and migraine-like episodes. *Epilepsy Res.*, **85**, 118–122.
16. Sirerol-Piquer, M.S., Ayerdi-Izquierdo, A., Morante-Redolat, J.M., Herranz-Perez, V., Favell, K., Barker, P.A. and Perez-Tur, J. (2006) The epilepsy gene LGI1 encodes a secreted glycoprotein that binds to the cell surface. *Hum. Mol. Genet.*, **15**, 3436–3445.
17. Striano, P., de Falco, A., Diani, E., Bovo, G., Furlan, S., Vitiello, L., Pinardi, F., Striano, S., Michelucci, R., de Falco, F.A. *et al.* (2008) A novel loss-of-function LGI1 mutation linked to autosomal dominant lateral temporal epilepsy. *Arch. Neurol.*, **65**, 939–942.
18. Di Bonaventura, C., Operto, F.F., Busolin, G., Egeo, G., D'Aniello, A., Vitello, L., Smaniotto, G., Furlan, S., Diani, E., Michelucci, R. *et al.* (2011) Low penetrance and effect on protein secretion of LGI1 mutations causing autosomal dominant lateral temporal epilepsy. *Epilepsia*, **52**, 1258–1264.
19. Silva, J., Wang, G. and Cowell, J.K. (2011) The temporal and spatial expression pattern of the LGI1 epilepsy predisposition gene during mouse embryonic cranial development. *BMC Neurosci.*, **12**, 43.
20. Chabrol, E., Navarro, V., Provenzano, G., Cohen, I., Dinocourt, C., Rivaud-Pechoux, S., Fricker, D., Baulac, M., Miles, R., Leguern, E. *et al.* (2010) Electroclinical characterization of epileptic seizures in leucine-rich, glioma-inactivated 1-deficient mice. *Brain*, **133**, 2749–2762.
21. Zhou, Y.D., Lee, S., Jin, Z., Wright, M., Smith, S.E. and Anderson, M.P. (2009) Arrested maturation of excitatory synapses in autosomal dominant lateral temporal lobe epilepsy. *Nat. Med.*, **15**, 1208–1214.
22. Schulte, U., Thumfart, J.O., Klocker, N., Sailer, C.A., Bildl, W., Biniossek, M., Dehn, D., Deller, T., Eble, S., Abbass, K. *et al.* (2006) The epilepsy-linked Lgi1 protein assembles into presynaptic Kv1 channels and inhibits inactivation by Kvbeta1. *Neuron*, **49**, 697–706.
23. Fukata, Y., Adesnik, H., Iwanaga, T., Bredt, D.S., Nicoll, R.A. and Fukata, M. (2006) Epilepsy-related ligand/receptor complex LGI1 and ADAM22 regulate synaptic transmission. *Science*, **313**, 1792–1795.
24. Sagane, K., Ishihama, Y. and Sugimoto, H. (2008) LGI1 and LGI4 bind to ADAM22, ADAM23 and ADAM11. *Int. J. Biol. Sci.*, **4**, 387–396.
25. Thomas, R., Favell, K., Morante-Redolat, J., Pool, M., Kent, C., Wright, M., Daignault, K., Ferraro, G.B., Montcalm, S., Durocher, Y. *et al.* (2010) LGI1 is a Nogo receptor 1 ligand that antagonizes myelin-based growth inhibition. *J. Neurosci.*, **30**, 6607–6612.
26. Fukata, Y., Lovero, K.L., Iwanaga, T., Watanabe, A., Yokoi, N., Tabuchi, K., Shigemoto, R., Nicoll, R.A. and Fukata, M. (2010) Disruption of LGI1-linked synaptic complex causes abnormal synaptic transmission and epilepsy. *Proc. Natl Acad. Sci. USA*, **107**, 3799–3804.
27. Yu, Y.E., Wen, L., Silva, J., Li, Z., Head, K., Sossey-Alaoui, K., Pao, A., Mei, L. and Cowell, J.K. (2010) Lgi1 null mutant mice exhibit myoclonic seizures and CA1 neuronal hyperexcitability. *Hum. Mol. Genet.*, **19**, 1702–1711.
28. Zhou, Y.D., Zhang, D., Ozkaynak, E., Wang, X., Kasper, E.M., Leguern, E., Baulac, S. and Anderson, M.P. (2012) Epilepsy gene LGI1 regulates postnatal developmental remodeling of retinogeniculate synapses. *J. Neurosci.*, **32**, 903–910.
29. Mashimo, T., Yanagihara, K., Tokuda, S., Voigt, B., Takizawa, A., Nakajima, R., Kato, M., Hirabayashi, M., Kuramoto, T. and Serikawa, T.

(2008) An ENU-induced mutant archive for gene targeting in rats. *Nat. Genet.*, **40**, 514–515.
30. Ross, K.C. and Coleman, J.R. (2000) Developmental and genetic audiogenic seizure models: behavior and biological substrates. *Neurosci. Biobehav. Rev.*, **24**, 639–653.
31. Leonardi, E., Andreazza, S., Vanin, S., Busolin, G., Nobile, C. and Tosatto, S.C.E. (2011) A computational model of the LGI1 protein suggests a common binding site for ADAM proteins. *PLoS One*, **6**, e18142.
32. Owuor, K., Harel, N.Y., Englot, D.J., Hisama, F., Blumenfeld, H. and Strittmatter, S.M. (2009) LGI1-associated epilepsy through altered ADAM23-dependent neuronal morphology. *Mol. Cell. Neurosci.*, **42**, 448–457.
33. Lynch, B.A., Lambeng, N., Nocka, K., Kensel-Hammes, P., Bajjalieh, S.M., Matagne, A. and Fuks, B. (2004) The synaptic vesicle protein SV2A is the binding site for the antiepileptic drug levetiracetam. *Proc. Natl Acad. Sci. USA*, **101**, 9861–9866.
34. Kaminski, R.M., Gillard, M., Leclercq, K., Hanon, E., Lorent, G., Dassesse, D., Matagne, A. and Klitgaard, H. (2009) Proepileptic phenotype of SV2A-deficient mice is associated with reduced anticonvulsant efficacy of levetiracetam. *Epilepsia*, **50**, 1729–1740.
35. Kunapuli, P., Jang, G.F., Kazim, L. and Cowell, J.K. (2009) Mass spectrometry identifies LGI1-interacting proteins that are involved in synaptic vesicle function in the human brain. *J. Mol. Neurosci.*, **39**, 137–143.
36. McCutcheon, J.E. and Marinelli, M. (2009) Age matters. *Eur. J. Neurosci.*, **29**, 997–1014.
37. Sagane, K., Hayakawa, K., Kai, J., Hirohashi, T., Takahashi, E., Miyamoto, N., Ino, M., Oki, T., Yamazaki, K. and Nagasu, T. (2005) Ataxia and peripheral nerve hypomyelination in ADAM22-deficient mice. *BMC Neurosci.*, **6**, 33.
38. Smart, S.L., Lopantsev, V., Zhang, C.L., Robbins, C.A., Wang, H., Chiu, S.Y., Schwartzkroin, P.A., Messing, A. and Tempel, B.L. (1998) Deletion of the K(V)1.1 potassium channel causes epilepsy in mice. *Neuron*, **20**, 809–819.
39. Yu, F.H., Mantegazza, M., Westenbroek, R.E., Robbins, C.A., Kalume, F., Burton, K.A., Spain, W.J., McKnight, G.S., Scheuer, T. and Catterall, W.A. (2006) Reduced sodium current in GABAergic interneurons in a mouse model of severe myoclonic epilepsy in infancy. *Nat. Neurosci.*, **9**, 1142–1149.
40. Ross, K.C. and Coleman, J.R. (1999) Audiogenic seizures in the developmentally primed Long-Evans rat. *Dev. Psychobiol.*, **34**, 303–313.

Biochemical and Biophysical Research Communications 418 (2012) 553–558

Contents lists available at SciVerse ScienceDirect

Biochemical and Biophysical Research Communications

journal homepage: www.elsevier.com/locate/ybbrc

Hypercholesterolemia and atherosclerosis in low density lipoprotein receptor mutant rats

Makoto Asahina [a,*], Tomoji Mashimo [b], Michiyasu Takeyama [a], Ryuichi Tozawa [a], Tadatoshi Hashimoto [a], Akiko Takizawa [b], Masatsugu Ueda [c], Toshihiro Aoto [c], Takashi Kuramoto [b], Tadao Serikawa [b]

[a] Takeda Pharmaceutical Company Ltd., Pharmaceutical Research Division, Kanagawa, Japan
[b] Kyoto University, Graduate School of Medicine, Institute of Laboratory Animals, Kyoto, Japan
[c] PhoenixBio Co., Ltd., Tochigi, Japan

ARTICLE INFO

Article history:
Received 21 December 2011
Available online 24 January 2012

Keywords:
LDLR
ENU-mutagenesis
Rats
Hypercholesterolemia
Atherosclerosis

ABSTRACT

To establish low density lipoprotein receptor (LDLR) mutant rats as a hypercholesterolemia and atherosclerosis model, we screened the rat LDLR gene for mutations using an *N*-ethyl-*N*-nitrosourea mutagenesis archive of rat gene data, and identified five mutations in its introns and one missense mutation (478T > A) in exon 4. The C160S mutation was located in the ligand binding domain of LDLR and was revealed to be equivalent to mutations (C160Y/G) identified in human familial hypercholesterolemia (FH) patients. The wild type, heterozygous, and homozygous mutant rats were fed a normal chow diet or a high fat high cholesterol (HFHC) diet from the age of 10 weeks for 16 weeks. The LDLR homozygous mutants fed the normal chow diet showed higher levels of plasma total cholesterol and LDL cholesterol than the wild type rats. When fed the HFHC diet, the homozygous mutant rats exhibited severe hyperlipidemia and significant lipid deposition from the aortic arch to the abdominal aorta as well as in the aortic valves. Furthermore, the female homozygous mutants also developed xanthomatosis in their paws. In conclusion, we suggest that LDLR mutant rats are a useful novel animal model of hypercholesterolemia and atherosclerosis.

1. Introduction

Cardiovascular disease, which is the leading cause of mortality in developed countries, is mainly caused by atherosclerosis. It is widely accepted that hypercholesterolemia, and especially an increase in the serum concentration of low density lipoprotein cholesterol (LDL-C), is a major risk factor for atherosclerosis in humans. The LDL receptor (LDLR) plays a key role in LDL metabolism, which involves the endocytosis and degradation of LDL and mainly occurs in the liver [1]. Therefore, LDLR dysfunction leads to the retention of LDL-C in the circulating blood and lipid deposition in the vascular walls, eventually causing atherosclerosis. Actually, familial hypercholesterolemia (FH) patients with defective LDLR display high plasma levels of LDL-C and are at significant risk of developing cardiovascular disease [2,3]. Likewise, LDLR knockout mice [4], LDLR mutant mice [5], and Watanabe heritable hyperlipidemia (WHHL) rabbits [6] have been established and widely used as well-validated animal models of hypercholesterolemia and atherosclerosis. However, there have been no reports of rat hypercholesterolemia and atherosclerosis models that display LDLR dysfunction, and furthermore, only two hyperlipidemic/atherosclerotic rat models have been reported, Dahl salt-sensitive hypertensive CETP transgenic (Tg[hCETP]DS) rats [7] and JCL:LA-cp rats [8].

Rat species have been widely used for various physiological studies because they are large enough to allow surgical operations to be performed on them and to allow evaluations of their cardiovascular function. In addition, it is possible to obtain larger biological samples from rats than from mice [9]. The strong reproductive performance of rats also results in a lower breeding cost, and they require less space than rabbits. Furthermore, there are many established rat metabolic disease models, which develop hypertension, obese, diabetes, hyperlipidemia, and combinations of these diseases [10,11], which are also major risk factors for atherosclerosis. Thus, a rat model would be an attractive option for investigating not only the interaction between metabolic disease and atherosclerosis but also their effects on cardiovascular outcomes.

In this study, we screened LDLR mutant rats as a novel hypercholesterolemia and atherosclerosis model using a gene-driven *N*-ethyl-*N*-nitrosourea (ENU) mutagenesis archive of the F344/NSlc rat genome, the Kyoto University Rat Mutant Archive (KURMA)

* Corresponding author. Address: Biological Research Laboratories, Pharmaceutical Research Division, Takeda Pharmaceutical Company Ltd., 26-1, Muraokahigashi 2chome, Fujisawa, Kanagawa 251-8555, Japan. Fax: +81 4 6629 4438.
E-mail address: Asahina_makoto@takeda.co.jp (M. Asahina).

0006-291X/$ - see front matter © 2012 Elsevier Inc. All rights reserved.
doi:10.1016/j.bbrc.2012.01.067

[12]. The KURMA is composed of sperm and DNA samples from more than 5000 G1 rats, and the number of G1 sperm and DNA samples has been increasing, which has allowed us to identify mutations in a wide variety of genes [12]. Previously, KURMA projects have efficiently produced a variety of rat mutants by combining a high-throughput screening technique and the intracytoplasmic sperm injection (ICSI) technique [13–15]. The present study will show that the LDLR mutant rat is a novel animal model of hypercholesterolemia, aortic atherosclerosis, and xanthoma that develops similar symptoms to FH patients.

2. Materials and methods

All animal care procedures and experiments conformed to the Guidelines for Animal Experiments at Kyoto University and were approved by both the Animal Research Committee of Kyoto University and the Experimental Animal Care and Use Committee of Takeda Pharmaceutical Company Limited.

2.1. Establishment of LDLR mutant rats

A total of 4608 DNA samples from ENU-mutagenized F344/Slc rats (Japan SLC Inc.), which were obtained from the KURMA, were screened with 14 primer sets, which were designed to amplify all exons and some introns of the rat LDLR gene (GenBank ID: 300438) (Supplementary Table 1). The protocols used for MuTPOWER screening of the KURMA were described previously [12]. Then, rats carrying a mutation in the LDLR gene were produced by the ICSI of frozen sperm into the eggs of female F344/NSlc rats [12]. The LDLR mutant rats will be deposited in the National BioResource Project – Rat in Japan and will be available from the Project (http://www.anim.med.kyoto-u.ac.jp/nbr).

2.2. Animals

ENU-mutagenesis of the samples in the KURMA usually introduces a few hundred random mutations per genome in rats [12]. Therefore, male rats carrying the LDLR gene mutation were backcrossed three times with female F344/NSlc rats to remove the residual mutations induced by ENU. The N3F1 littermates of the wild type, heterozygous, and homozygous mutants were obtained by cross breeding them with their N3 littermates and were used to validate the effect of the LDLR gene mutation. Furthermore, F344/NSlc rats, the original rat strain used to produce the KURMA, were compared with wild type rats to confirm the effect of off-target mutations in LDLR mutant rats. All rats were housed in a room under controlled temperature (23 °C), humidity (55%), and lighting conditions (lights on from 7:30 am to 7:30 pm) and were fed a normal chow diet (CE2 diet, CLEA Japan) or a high fat high cholesterol (HFHC) diet (Research Diet, D12336) from the age of 10 weeks for 4 months and were allowed free access to water.

Genotyping of the T478A mutation was performed using allele specific PCR based TaqMan assays (forward primer: 5′-TGCTCACT TCCGCTGCAA-3′, reverse primer: 5′-GCAGGCCCACAGGCT-3′, FAM reporter: CTCCTCTTCCTGCATCC, VIC reporter: CCTCTTCCAGCATCC) designed by Applied Biosystems, according to the manufacturer's protocol on a 7900HT Fast Real-Time PCR system (Applied Biosystems).

2.3. Plasma lipids profiles

Blood samples were collected from the tail vein with EDTA (Wako Pure Chemicals) used as an anticoagulant. Plasma high density lipoproteins (HDL) were fractionated by precipitation using a commercially available kit (Wako Pure Chemicals). Then, plasma total cholesterol, HDL cholesterol (HDL-C), and the triglyceride (TG) level were measured using enzymatic assay reagents (Wako Pure Chemicals). The plasma lipoprotein profiles of pooled plasma samples from the rats in each group ($n = 7$) were analyzed by an online dual enzymatic method for the simultaneous quantification of cholesterol by high-performance liquid chromatography (HPLC) (Skylight Biotech Inc.).

2.4. Atherosclerotic lesion analysis

Twenty-six-week-old rats, which were fed the normal chow diet or the HFHC diet from the age of 10 weeks, were sacrificed, and their hearts and aortas were fixed in 10% neutral formaldehyde solution after the removal of connective tissue. The aorta was opened longitudinally, stained with oil red O, and imaged using a digital camera. The oil red O-positive area was calculated using Image-Pro Plus™ (Media Cybernetics) and was expressed as a percentage of the total surface area. For the evaluation of cross sections of the aortic sinus and abdominal aorta, 100-μm cross sections of the aortic roots were prepared at the position of the

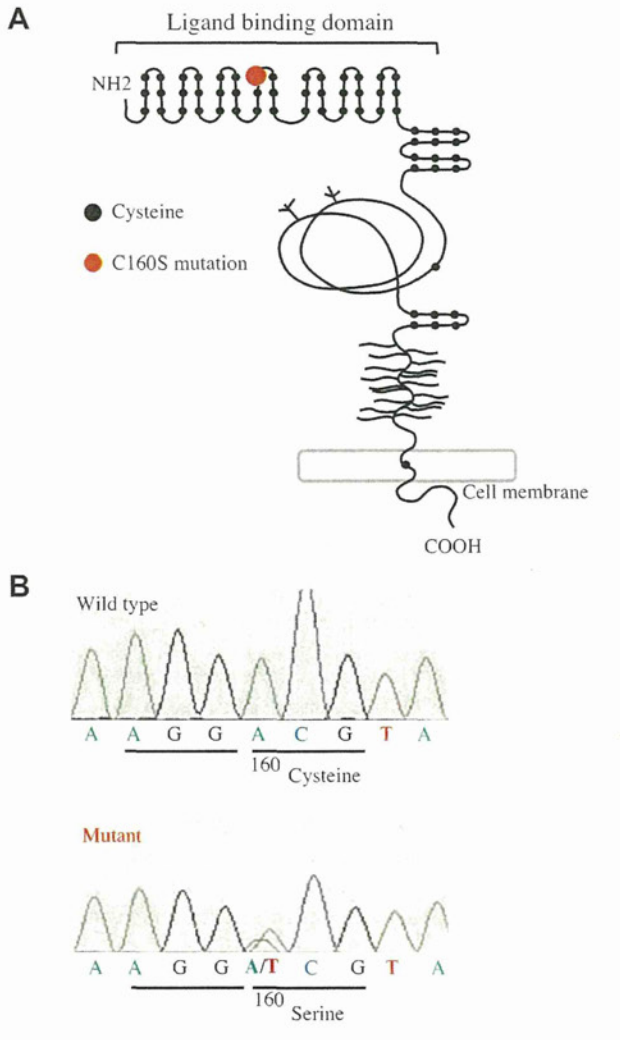

Fig. 1. Establishment of LDLR mutant rats. (A) Schematic diagram showing the ligand binding domain of the LDLR. The C160S mutation was located in the ligand binding domain of the LDLR. (B) Sequencing of the LDLR gene of the F1 mutant rats confirmed that the C160S mutation was present.

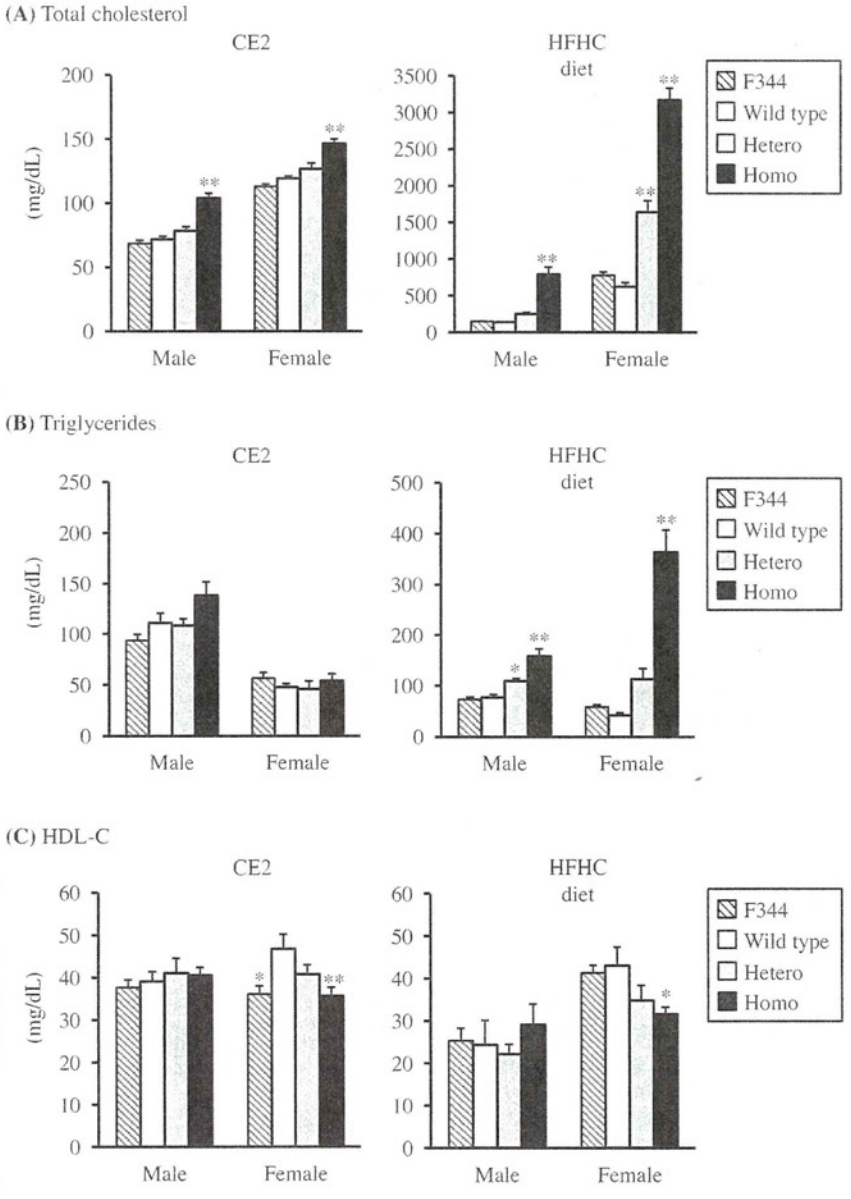

Fig. 2. Plasma lipids (A: Total cholesterol, B: Triglyceride, C: HDL-c) concentrations in the F344, wild type, and heterozygous (hetero) and homozygous (homo) mutant rats fed the normal chow or HFHC diet. The asterisks indicate a significant difference at $^{*}P < 0.05$ or $^{**}P < 0.01$ compared with the wild type.

aortic valves using a cryostat and stained with hematoxylin and eosin (H and E) or oil red O.

2.5. Quantitative real time PCR

Twenty-six-week-old rats were sacrificed after being fed the normal chow diet for 16 weeks, and the total RNA in their liver was extracted with the ISOGEN kit (NipponGene). The RNA was treated with DNase I (Wako Pure Chemical). Then, first-strand cDNA was synthesized using the SuperScript III cDNA synthesis kit (Invitrogen). We carried out real-time quantitative PCR to assess the mRNA expression levels of LDLR and glycerol-3-phosphate dehydrogenase (GAPD) in the liver using the 7900HT Fast Real-Time PCR system with commercial Taqman probe kits, TaqMan Gene Expression Assays (GenBank ID: 300438 and 24383, respectively), and Taqman Universal PCR Master Mix (Applied Biosystems), according to the manufacturer's instructions. GAPD was used as a housekeeping reference gene.

2.6. Statistical analysis

Statistical significance was determined using the Student's *t*-test for comparisons between two groups or Dunnett's test for comparisons of plasma lipid levels and atherosclerotic lesion areas among the littermates of the LDLR mutant rats. All data are shown as the mean ± standard error (SEM). $^{*}P < 0.05$ and $^{**}P < 0.01$ were defined as significant.

3. Results

3.1. Establishment of LDLR mutant rats

By screening all the exons and some of the introns of the LDLR gene using about 5000 DNA samples from the KURMA, five mutations were identified in its introns and one missense mutation (478T > A) was found in exon 4 (Supplementary Table 2). This

478T > A missense mutation resulted in the amino acid substitution of the 160th cysteine for serine. The 160th cysteine was located in the cysteine-rich ligand binding domain of the LDLR (Fig. 1A). Rats carrying this mutation were produced using the corresponding frozen sperm. The missense mutation was confirmed to be present in these animals, which were F1 hybrids between F344/NSlc and G1 donor rats (Fig. 1B). Expression analyses showed that the hepatic expression of LDLR mRNA in the homozygous mutant was not significantly altered compared with that in their wild type littermates (F344 100 ± 14, Wild type 72 ± 9, Homo 67 ± 7, Hepatic mRNA levels of LDLR quantified by real-time quantitative PCR in male rats fed a normal chow diet for 4 months ($n = 6$). The results are expressed as relative values compared to GAPD mRNA expression. The values are shown as the mean ± SEM.). No prominent behavioral abnormalities, appearance defects, or reproductive problems were observed in the LDLR mutant rats.

3.2. Plasma lipids profiles

The LDLR homozygous mutants fed the normal chow diet exhibited higher total plasma cholesterol levels and an increased LDL cholesterol fraction compared with the wild type rats (both sexes). (Figs. 2A and 3A), whereas no significant difference in plasma total cholesterol and TG levels was observed between the wild type and F344 rats. But, compared with the female wild type rats, the female F344 rats showed significantly decreased plasma HDL-C levels only in the normal diet-fed conditions (Fig. 2C). In the rats fed the HFHC diet for 4 months, the homozygous mutants exhibited markedly increased plasma total cholesterol levels compared with the wild type rats (both sexes) (Fig. 2A), and the intermediate fraction between VLDL and LDL was the most common type of lipoprotein in the LDLR homozygous mutant rats (Fig. 3B).

Regardless of their diet conditions and genotype, the female mutant rats showed severe hypercholesterolemia compared to the male rats (Fig. 2A), and the male mutant rats exhibited no significant alterations in their plasma HDL-C levels in either diet conditions, whereas the female homozygous mutant rats showed significantly decreased plasma HDL-C levels compared with those of the wild type rats in the normal and HFHC diet-fed conditions (Fig. 2C). Furthermore, there was no significant difference in plasma TG levels among either genotype of either sex in the normal chow diet-fed conditions, whereas the homozygous mutant rats fed the HFHC diet showed significantly increased plasma TG levels compared with the wild type rats, especially the female rats (Fig. 2B), indicating that a sex difference in plasma lipid metabolism existed in the LDLR mutant rats.

3.3. Atherosclerotic lesions and xanthoma

Both the male and female LDLR homozygous mutants fed the HFHC diet for 4 months showed lipid deposition from the thoracic to abdominal aorta (Fig. 4A and B). The female homozygous mutants showed more severe aortic atherosclerotic lesions than the male homozygous mutant rats. The female F344 and wild type rats also showed slight lipid deposition in the aorta, while no lesions were detected in the male F344 or wild type rats (Fig. 4A and B).

A histological examination of the abdominal aortae of the female rats maintained on the HFHC diet for 4 months showed slight lipid deposition in the vascular endothelium (Fig. 4C). Histological sections of the aortic sinuses of the male and female homozygous LDLR mutant rats fed the HFHC diet demonstrated lipid deposition (Fig. 4D).

The female homozygous mutants also exhibited xanthoma in their hind paws, while no xanthoma was observed in the male homozygous mutants (Fig. 4E).

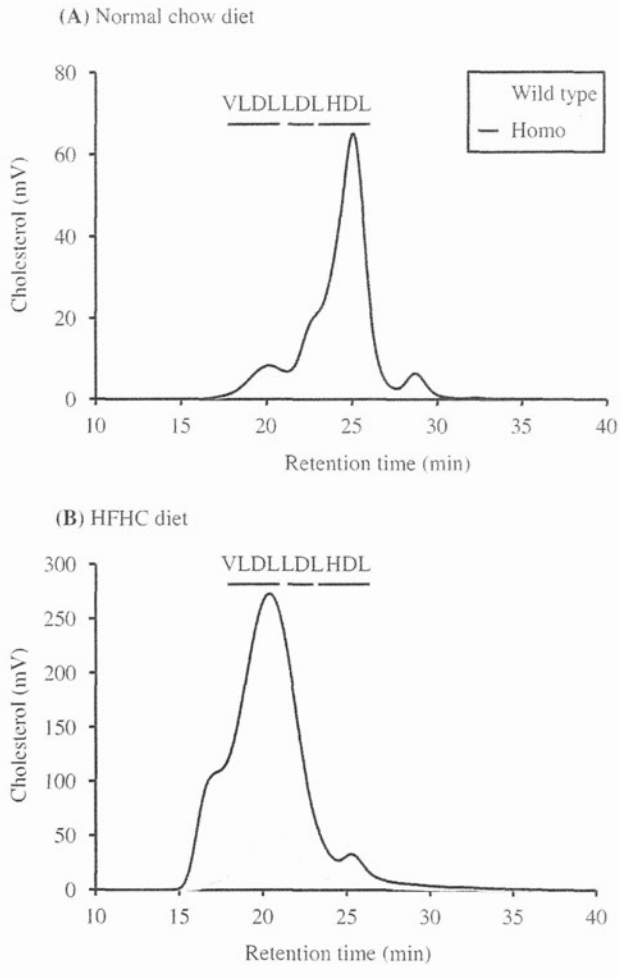

Fig. 3. Lipoprotein profiles of male LDL receptor mutant rats. Pooled plasma samples from male wild type and homozygous mutant rats ($n = 7$) were fractionated by HPLC, and their cholesterol levels were determined by an online dual enzymatic method. The rats were fed the normal chow (A) or HFHC diet (B) for 4 months.

4. Discussion

Although LDLR mutant mice harboring the C699Y mutation in the LDLR have previously been generated by ENU-mutagenesis [5], we were the first to establish LDLR mutant rats carrying the amino acid substitution C160S in the ligand binding domain of LDLR by ENU-mutagenesis. In this study, the LDLR mutant rats displayed hypercholesterolemia, aortic atherosclerosis, and xanthomatosis in their limbs, which are typical phenotypes of human FH patients, LDLR knockout mice, and WHHL rabbits.

The C160S mutation in the rat LDLR, which was detected by KURMA screening, was located in exon 4 of the LDLR genome, within the ligand binding domain of the LDLR protein, which consists of seven successive cysteine-rich repeats. This cysteine mutation is expected to affect the conformation of the LDLR protein by breaking the S–S bond of cysteine. The hepatic expression of LDLR mRNA in the homozygous mutant was not significantly altered compared with that of its wild-type littermates, and similar results were obtained for LDLR protein expression in the liver (data not shown). Therefore, an impairment of the LDL catabolic activity of the LDLR might cause the hypercholesterolemia observed in LDLR mutant rats. Actually, the mutation of the 160th cysteine of the LDLR possessed by the LDLR mutant rats is comparable to the C160S mutation found in human FH patients [16].

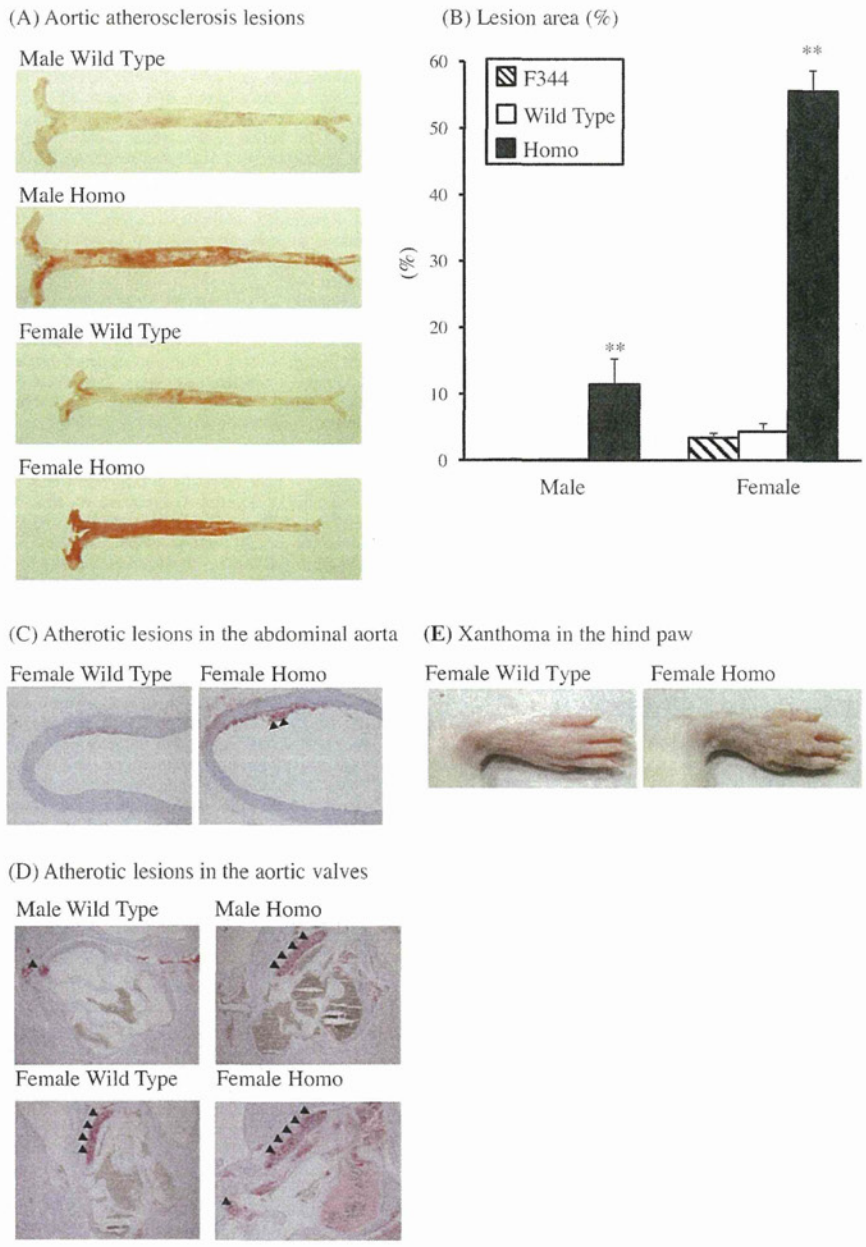

Fig. 4. Atherosclerotic lesions and xanthoma in 26-week-old LDLR mutant rats maintained on the HFHC diet for 4 months. The filled triangles show oil-red O stain positive areas. (A) Aortic atherosclerotic lesions in the wild type and homozygous mutant rats (both sexes). (B) Aortic atherosclerosis lesion area in male and female rats. The asterisk indicates a significant difference at $^{**}P < 0.01$ compared with the wild type rats. (C) Histological sections of the abdominal aorta from female wild type rats and homozygous mutant rats. (D) Histological sections of the aortic valves from wild type rats and homozygous mutant rats (both sexes). (E) Xanthoma of the hind paws in female homozygous mutant rats.

Unlike FH patients and other LDLR deficient animals including LDLR knockout mice [4] and WHHL rabbits [17], the LDLR mutant rats exhibited significant sex differences in the severity of their dyslipidemia and atherosclerosis. The female homozygous mutant rats showed plasma total cholesterol levels that were approximately three times higher than those of the male homozygous mutants and exhibited more severe atherosclerosis and xanthoma than the male homozygous mutants. Generally, female rats secrete more VLDL than male rats [18–20], but this is not the case for C57BL mice [21]. A previous study also showed that the microsomal triglyceride transfer protein (MTP) expression levels of male Sprague Dawley rats were about 40% lower than those of female rats [22]. MTP is crucial for the assembly and secretion of apolipoproteinB (apoB)-containing lipoproteins. Heterozygous MTP knockout mice, which display a 50% reduction in their MTP expression, demonstrate decreased secretion and plasma levels of apoB-containing lipoproteins [23,24]. Therefore, the observed sex difference in the blood lipid profiles of the LDLR mutant rats might depend on their MTP expression levels.

However, in the HFHC diet conditions, the male homozygous mutant rats showed significantly more severe atherosclerotic lesions ($P < 0.05$) than the female wild type rats, which showed comparable plasma total cholesterol and HDL-C levels to the male homozygous mutant rats. Previous studies suggested that estrogen

plays a protective role against the progression of atherosclerosis independently of plasma cholesterol levels in humans and mice [25]. Therefore, it is suggested that the atherosclerotic lesion area might have been affected by sex-hormones in the female F344 rats. Furthermore, the male homozygous mutant rats showed higher plasma TG levels than the female wild type rats in this study ($P < 0.05$). Ovariectomized mice also showed increased numbers of atherosclerotic lesions and higher plasma TG levels than sham-operated mice, although there was no significant difference in plasma cholesterol levels between them [26]. Therefore, it is suggested that estrogen has direct or indirect anti-atherogenic effects on plasma TG levels in female F344 rats.

In humans, atherosclerotic lesions are frequently observed in the abdominal aorta and coronary arteries [27], but Jackson et al. found that small rodent models such as mice and rats suffer from the limitation that they usually develop atherosclerotic lesions in non-coronary vessels [28]. Actually, the LDLR mutant rats also exhibited significant atherosclerotic lesions in their thoracic and abdominal aorta, but no lesions in their coronary arteries in the present experimental conditions (data not shown). However, some rat atherosclerosis models such as Tg[hCETP]DS rats [7] and JCR:LA-cp rats [8], which display multiple risk factors for cardiovascular events, including dyslipidemia, hypertension, obesity, and diabetes, exhibit atherosclerotic lesions in their coronary arteries and myocardial infarction. Therefore, LDLR mutant rats, which develop multiple diseases associated with cardiovascular events, might be a novel cardiovascular model that develop atherosclerosis in their coronary arteries.

This study is the first report about LDLR mutant rats, which spontaneously develop dyslipidemia, atherosclerosis, and xanthoma. Compared with mice and rabbits, rats are a more appropriate size for various physiological studies. Therefore, LDLR mutant rats would be a useful animal model for studying lipid metabolism, atherosclerosis, and cardiovascular disease.

Disclosures

None.

Acknowledgments

LDLR mutant rat strain, which is named as F344-*Ldlr*^{mkyo}/Ta will be deposited in the National BioResource Project – Rat in Japan and is available from the Project (http://www.anim.med.kyoto-u.ac.jp/nbr).

Appendix A. Supplementary material

Supplementary data associated with this article can be found, in the online version, at doi:10.1016/j.bbrc.2012.01.067.

References

[1] M.S. Brown, J.L. Goldstein, How LDL receptors influence cholesterol and atherosclerosis, Sci. Am. 251 (1984) 58–66.
[2] H. Mabuchi, J. Koizumi, M. Shimizu, R. Takeda, Development of coronary heart disease in familial hypercholesterolemia, Circulation 79 (1989) 225–232.
[3] H. Mabuchi, T. Haba, K. Ueda, R. Ueda, R. Tatami, S. Ito, T. Kametani, J. Koizumi, S. Miyamoto, M. Ohta, R. Takeda, T. Takegoshi, H. Takeshita, Serum lipids and coronary heart disease in heterozygous familial hypercholesterolemia in the Hokuriku District of Japan, Atherosclerosis 28 (1977) 417–423.
[4] S. Ishibashi, J.L. Goldstein, M.S. Brown, J. Herz, D.K. Burns, Massive xanthomatosis and atheroclerosis in cholesterol-fed low density lipoprotein receptor-negative mice, J. Clin. Invest. 93 (1994) 1885–1893.
[5] K.L. Svenson, N. Ahituv, R.S. Durgin, H. Savage, P.A. Magnani, O. Foreman, B. Paigen, L.L. Peters, A new mouse mutant for the LDL receptor identified using ENU mutagenesis, J. Lipid Res. 49 (2008) 2452–2462.
[6] Y. Watanabe, Serial inbreeding of rabbits with hereditary hyperlipidemia (WHHL-rabbit), Atherosclerosis 36 (1980) 261–268.
[7] V.L. Herrera, S.C. Makrides, H.X. Xie, H. Adari, R.M. Krauss, U.S. Ryan, N. Ruiz-Opazo, Spontaneous combined hyperlipidemia, coronary heart disease and decreased survival in Dahl salt-sensitive hypertensive rats transgenic for human cholesteryl ester transfer protein, Nat. Med. 5 (1999) 1383–1389.
[8] J.C. Russell, S.E. Graham, M. Richardson, Cardiovascular disease in the JCR:LA-cp rat, Mol. Cell. Biochem. 188 (1998) 113–126.
[9] P.M. Iannaccone, H.J. Jacob, Rats!, Dis Models Mech. 2 (2009) 206–210.
[10] Y.M. Pinto, M. Paul, D. Ganten, Lessons from rat models of hypertension: from Goldblatt to genetic engineering, Cardiovasc. Res. 39 (1998) 77–88.
[11] S.K. Panchal, L. Brown, Rodent models for metabolic syndrome research, J. Biomed. Biotechnol. 2011 (2011) 351982.
[12] T. Mashimo, K. Yanagihara, S. Tokuda, B. Voigt, A. Takizawa, R. Nakajima, M. Kato, M. Hirabayashi, T. Kuramoto, T. Serikawa, An ENU-induced mutant archive for gene targeting in rats, Nat. Genet. 40 (2008) 514–515.
[13] K. Yoshimi, T. Tanaka, A. Takizawa, M. Kato, M. Hirabayashi, T. Mashimo, T. Serikawa, T. Kuramoto, Enhanced colitis-associated colon carcinogenesis in a novel Apc mutant rat, Cancer Sci. 100 (2009) 2022–2027.
[14] T. Mashimo, I. Ohmori, M. Ouchida, Y. Ohno, T. Tsurumi, T. Miki, M. Wakamori, S. Ishihara, T. Yoshida, A. Takizawa, M. Kato, M. Hirabayashi, M. Sasa, Y. Mori, T. Serikawa, A missense mutation of the gene encoding voltage-dependent sodium channel (Nav1.1) confers susceptibility to febrile seizures in rats, J. Neurosci. 30 (2010) 5744–5753.
[15] T. Kuramoto, M. Kuwamura, F. Tagami, T. Mashimo, M. Nose, T. Serikawa, Kyoto rhino rats derived by ENU mutagenesis undergo congenital hair loss and exhibit focal glomerulosclerosis, Exp. Anim. 60 (2011) 57–63.
[16] I.N. Day, R.A. Whittall, S.D. O'Dell, L. Haddad, M.K. Bolla, V. Gudnason, S.E. Humphries, Spectrum of LDL receptor gene mutations in heterozygous familial hypercholesterolemia, Hum. Mutat. 10 (1997) 116–127.
[17] T. Ito, S. Yamada, M. Shiomi, Progression of coronary atherosclerosis relates to the onset of myocardial infarction in an animal model of spontaneous myocardial infarction (WHHLMI rabbits), Exp. Anim. 53 (2004) 339–346.
[18] M.L. Watkins, N. Fizette, M. Heimberg, Sexual influences on hepatic secretion of triglyceride, Biochim. Biophys. Acta 280 (1972) 82–85.
[19] W. Patsch, K. Kim, W. Wiest, G. Schonfeld, Effects of sex hormones on rat lipoproteins, Endocrinology 107 (1980) 1085–1094.
[20] C. Soler-Argilaga, A. Danon, H.G. Wilcox, M. Heimberg, Effects of sex on formation and properties of plasma very low density lipoprotein in vivo, Lipids 11 (1976) 517–525.
[21] B.J. van Vlijmen, H.B. van 't Hof, M.J. Mol, H. van der Boom, A. van der Zee, R.R. Frants, M.H. Hofker, L.M. Havekes, Modulation of very low density lipoprotein production and clearance contributes to age- and gender- dependent hyperlipoproteinemia in apolipoprotein E3-Leiden transgenic mice, J. Clin. Invest. 97 (1996) 1184–1192.
[22] C. Améen, J. Oscarsson, Sex difference in hepatic microsomal triglyceride transfer protein expression is determined by the growth hormone secretory pattern in the rat, Endocrinology 144 (2003) 3914–3921.
[23] M. Raabe, L.M. Flynn, C.H. Zlot, J.S. Wong, M.M. Veniant, R.L. Hamilton, S.G. Young, Knockout of the abetalipoproteinemia gene in mice. reduced lipoprotein secretion in heterozygotes and embryonic lethality in homozygotes, Proc. Natl. Acad. Sci. USA 95 (1998) 8686–8691.
[24] G.K. Leung, M.M. Veniant, S.K. Kim, C.H. Zlot, M. Raabe, J. Björkegren, R.A. Neese, M.K. Hellerstein, S.G. Young, Deficiency of microsomal triglyceride transfer protein reduces apolipoprotein B secretion, J. Biol. Chem. 275 (2000) 7515–7520.
[25] R.D. Patten, Models of gender differences in cardiovascular disease, Drug Discov. Today Dis. Models 4 (2007) 227–232.
[26] P.A. Bourassa, P.M. Milos, B.J. Gaynor, J.L. Breslow, R.J. Aiello, Estrogen reduces atherosclerotic lesion development in apolipoprotein E-deficient mice, Proc. Natl. Acad. Sci. USA 93 (1996) 10022–10027.
[27] J.F. Bentzon, E. Falk, Atherosclerotic lesions in mouse and man: is it the same disease?, Curr Opin. Lipidol. 21 (2010) 434–440.
[28] C.L. Jackson, U. Benbow, D.J. Galley, S. Karanam, Models of plaque rupture, Drug Discov. Today Dis. Models 4 (2007) 171–175.

トランスレーショナルリサーチを支援する

遺伝子医学 MOOK 22

Gene & Medicine

ISSN 1349-2527

最新疾患モデルと病態解明，創薬応用研究，細胞医薬創製研究の最前線

最新疾患モデル動物，ヒト化マウス，モデル細胞，ES・iPS細胞を利用した病態解明から創薬まで

【編　集】戸口田淳也
（京都大学iPS細胞研究所教授
京都大学再生医科学研究所教授）

池谷　真
（京都大学iPS細胞研究所准教授）

メディカルドゥ

2．ジンクフィンガーヌクレアーゼ（ZFN）による重症免疫不全（SCID）ラットの作製と創薬応用研究への試み

真下知士

ラットは，ヒト疾患モデルとしての利用価値が高く，薬理薬効試験，毒性試験にも多用される。近年，ジンクフィンガーヌクレアーゼ（ZFN）と呼ばれる人工ヌクレアーゼにより，これまで遺伝子改変技術がなかったラットにおいて，遺伝子改変を行うことが可能となった。本稿では，①ZFN技術を利用して開発した重症免疫不全（SCID）ラット，②SCIDラットにヒト細胞・組織などを移植したヒト化ラットについて紹介する。今後，人工ヌクレアーゼ技術により多数の疾患モデルラットが作製されるであろう。SCIDラットは，基礎・臨床医学研究，幹細胞移植研究，創薬研究などに有用なモデルになる。

はじめに

実験用ラットは，古くから医学，薬学，生物学，栄養学，行動学，心理学などの幅広い分野で利用されてきた。実験動物のもう1つの代表格であるマウスと並んで，遺伝的基盤と環境的基盤を厳格にコントロールしながら，実験を行うことができるメリットがある。さらに，ラットはマウスより体のサイズが10倍以上あるため，外科的処置実験，移植実験，生理実験，脳研究などに使われる。日本では1900年代初期から，ラット（シロネズミ）が実験動物として使用されていた記録が残っているが，以来，様々な疾患モデルラットが開発されてきた歴史がある。例えば，高血圧を自然に発症し脳卒中病変や心筋梗塞などヒト本態性高血圧によく似た症状を示す高血圧モデルSHRラット，インスリン分泌不全を呈するⅠ型糖尿病モデルKDPラット，自発性に強直性けいれんと欠神様発作を起こすてんかんモデルSERラットなど，世界中で利用されている優れた疾患モデルが開発されている。京都大学大学院医学研究科附属動物実験施設では，このような疾患モデルラットを収集して，研究者が効果的に利用できる研究基盤を整備する事業として，ナショナルバイオリソースプロジェクト「ラット」[用語1]を実施している[1]。収集されたラット系統は，ゲノムプロファイルと特性プロファイルを作製して，系統樹とともにユーザーフレンドリーなデータベースとして公開している。

図❶Aは，ラットとマウスの過去30年における研究論文数を比較した。これによると，約30年前は，ラットがマウスより約2倍ほど多く利用されていたが，2000年頃にほぼ同数となり，現在

key words
ラット，ナショナルバイオリソースプロジェクト，ジンクフィンガーヌクレアーゼ（ZFN），TALEヌクレアーゼ（TALEN），ノックアウトラット，遺伝子改変動物，重症複合免疫不全（SCID），ヒト化動物，担がん試験，人工多能性幹細胞（iPS細胞）

ではマウスの論文が約1.6倍報告されている。おそらくこれは，ノーベル医学生理学賞を受賞したマリオ・カペッキらによる胚性幹（ES）細胞を利用したノックアウト動物作製法（1989年）と関係していると思われる。これによりマウスでは，ES細胞を用いることで，特定の遺伝子を破壊した遺

図❶ ラットとマウスの論文数の比較

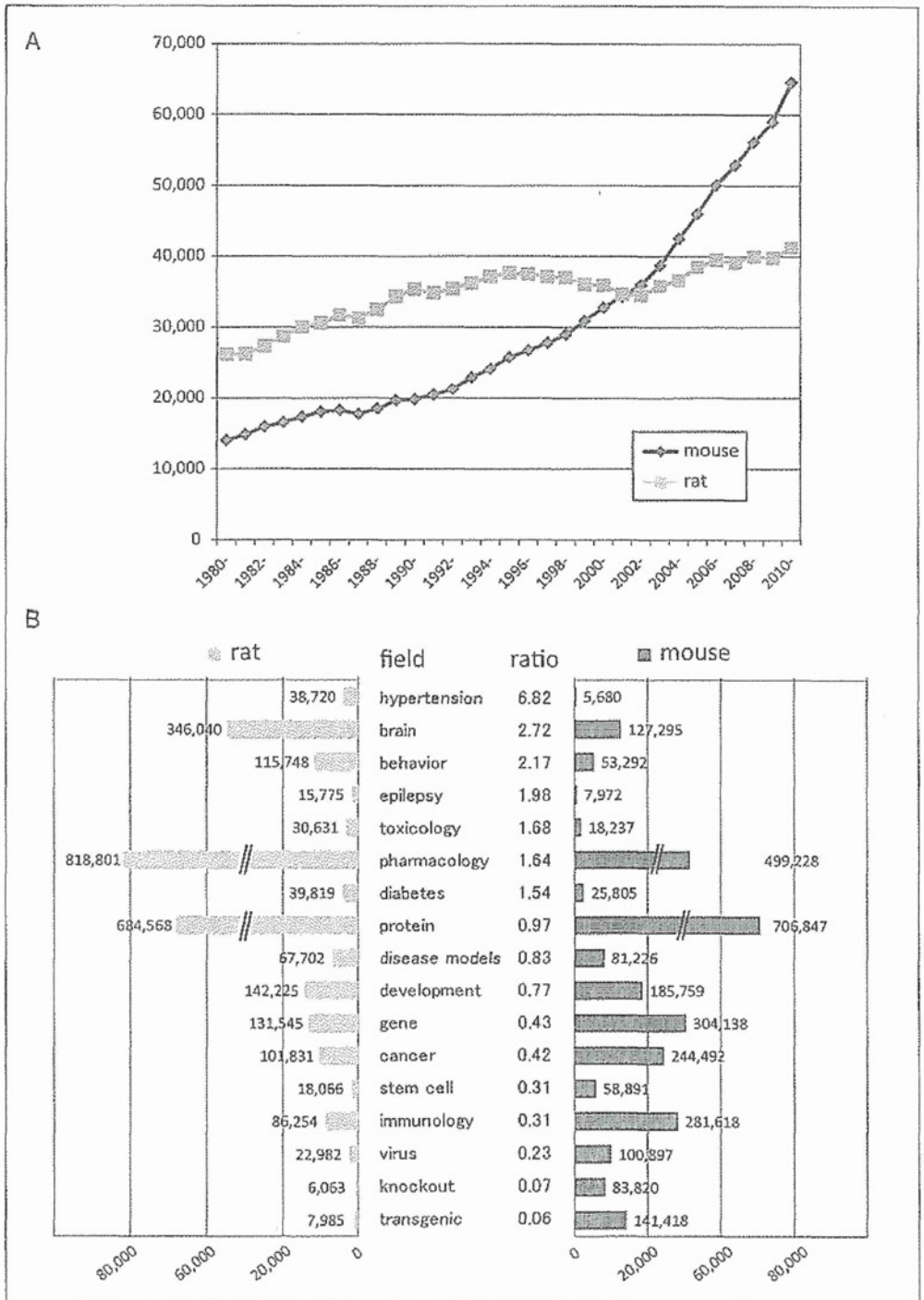

A. 過去30年におけるラットとマウスの研究論文数の比較。PubMed（http://www.ncbi.nlm.nih.gov/pubmed）から引用した。
B. ラットとマウスの利用分野の比較。グラフは論文数を表しており，ラット/マウス論文数の比率の順番に記してある。

伝子改変動物を作り，遺伝子の機能を調べることができるようになった。図❶Bは，マウスとラットがどのような研究分野で使われているかを表している。マウスはこの遺伝子操作技術の開発により，分子や遺伝子の働きを個体レベルで調べる研究が多く，がんや免疫などの研究に利用されている。一方ラットは，脳，神経系の分野で比較的多く使われている。ラットでは詳細な脳アトラスが作成されており，それに従い脳の特定の位置に電極を刺入したり，薬剤を注入したり，局部的に破壊することなどが可能である。高血圧や糖尿病の分野でラットが多く使われているのは，ヒトの病態に類似したモデルラットが開発されているのに加え，体のサイズが大きいので経時的採血や一度にたくさんの採血をすることが可能であり，詳細な生理学的測定を行うことができるからだろう。

このように実験用ラットは，マウスに比べていくつかの利点をもっているが，これまでES細胞がなかったためにノックアウトラットを作製することができなかった。最近になって，ようやくこのような状況が変わってきた。2010年，ノックアウトマウスが開発されてから21年の時を経て，ES細胞由来p53ノックアウトラットが報告された[2]。ラットES細胞のジャームラインストランスミッション効率は，マウスES細胞に比べると低く，培養条件や相同組換え技術などの改善がまだまだ必要である。最近，ES細胞とは全く異なる遺伝子改変技術として，ジンクフィンガーヌクレアーゼ（ZFN）[用語2]が細胞や植物，ゼブラフィッシュなどで報告された[3][4]。われわれはこのZFNを利用することで，X連鎖重症複合免疫不全症の原因遺伝子であるインターロイキン2受容体ガンマ鎖（*Il2rg*）のノックアウトラットを作製することに成功した[5]。

Ⅰ．ジンクフィンガーヌクレアーゼ（ZFN）

ジンクフィンガーヌクレアーゼ（ZFN）とは，DNA配列を特異的に認識するジンクフィンガータンパクと，DNAを切断するFokIヌクレアーゼを人工的に融合したタンパクのことである（図❷A）。1つの「ジンクフィンガー」ユニットは3bpのDNAに結合するため，3～6個の異なるジンクフィンガーユニットを組み合わせることで，9～18bpのDNA塩基配列を特異的に認識することができる。標的とするDNA配列に5～6bpを挟んでジンクフィンガーを2つデザインすることで，ジンクフィンガーに結合しているFokIヌクレアーゼが，挟まれた5～6bpのDNA領域に二本鎖切断を導入することができる（図❷B）。切断された二本鎖DNAは，通常，non-homologous end-joining（NHEJ）により修復されるが，この修復過程でしばしばDNA欠失（または挿入）変異が起こる。また，標的DNA配列に対して相同DNA配列が存在すると，相同組換えhomologous recombination（HR）が起きて，DNA配列が改変される。この過程は，理論的にはあらゆるDNA配列（あらゆる遺伝子）に適用できることから，人工的にデザインされたジンクフィンガーヌクレアーゼを用いることで，標的遺伝子を自由に破壊（ノックアウト）あるいは改変（ノックイン）することが可能となる。

ZFNを用いたノックアウトラットの作製方法を図❷Cに示す。ZFNs自体は，米国Sigma-Aldrich社から購入できる。あるいは，オープンリソースとして米国非営利団体Addgeneからライブラリーを購入して自分で作製することもできる。ZFNから動物を作製する方法は，ZFNs mRNAを利用する以外は，従来のトランスジェニック動物を作製する方法と同じである。これまでの報告では，ZFNs mRNAを注入して産まれてきたラットの約20～30%の個体に遺伝子変異が導入されている[5][6]。さらに，標的とするDNA配列に対して相同DNAプローブを利用することで，標的とする1塩基のDNA配列を改変することや，GFP遺伝子カセットをDNA配列特異的に挿入したノックインラットの作製が報告されている[7]。

ZFN技術は従来のES細胞技術に比べて，以下のようなメリットが挙げられる。通常，ES細胞を用いてノックアウト動物（マウス・ラット）を作製する場合は，ベクターの作製から個体作製まで約12～18ヵ月を要する。しかし，ZFN技術の場合には，ベクター作製，マイクロインジェクション，

図❷ ジンクフィンガーヌクレアーゼ（ZFN）

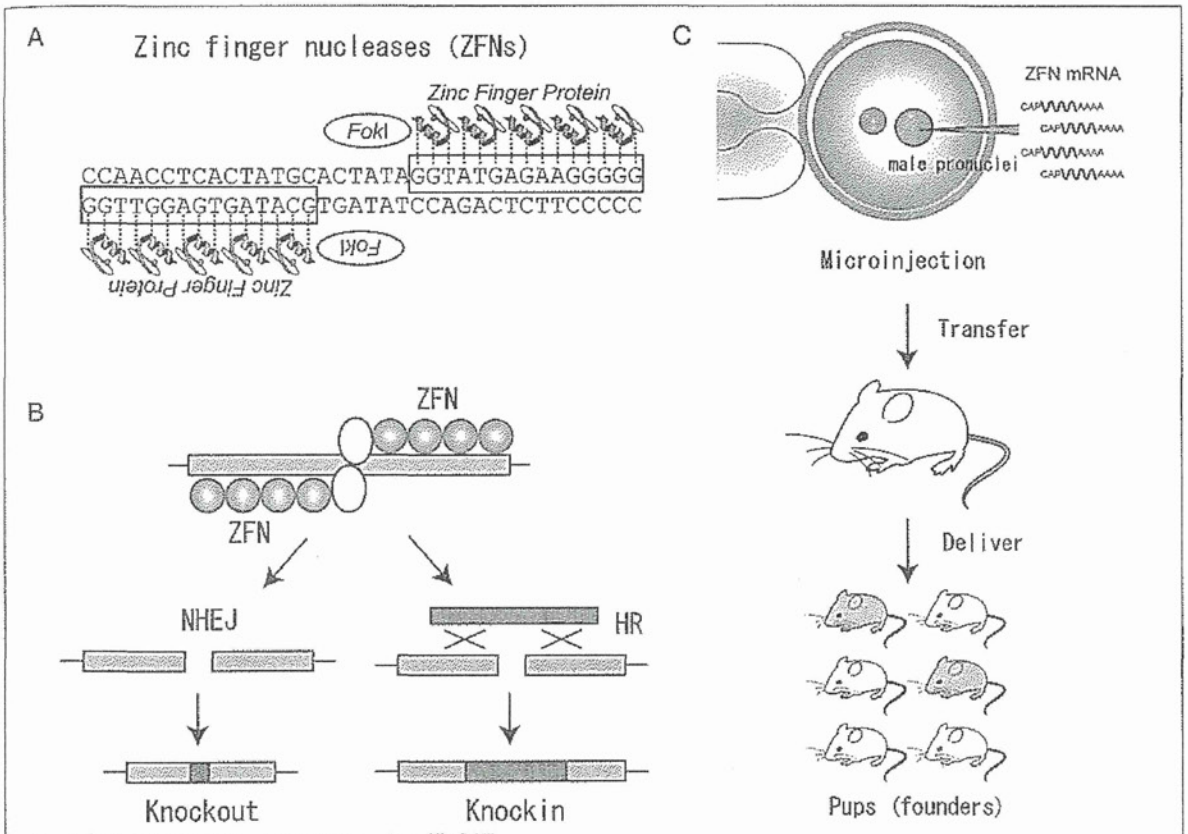

A. ジンクフィンガーヌクレアーゼの模式図
B. ジンクフィンガーヌクレアーゼによる標的遺伝子の認識および二本鎖DNAの切断。切断された二本鎖DNAは，非相同末端再結合（NHEJ）あるいは相同組換え（HR）により修復される。NHEJの場合には，数bpの遺伝子欠失が起こり（ノックアウト），HRの場合には遺伝子改変（ノックイン）が起こる。
C. ZFNsをマイクロインジェクション法により受精卵に注入することで，遺伝子改変ラットを作製することができる。

個体作製までに約6ヵ月で可能である。また，ダブル（トリプル）ノックアウト動物を簡単に作製することも可能である。ES細胞技術に比べて，遺伝子改変（ノックイン）動物の作製も容易に行える[7]。ES細胞による遺伝子改変は，ES細胞が確立された系統（マウスの場合，129系統やC57BL/6系統など）でしかできないが，ZFN技術はあらゆる系統について行うことができる。例えば，従来の疾患モデル動物に対して，遺伝子を破壊してさらに病気を起こしたり，逆に遺伝子を改変することで病気を治すことも可能となる。さらに，これまではES細胞がないために遺伝子改変動物を作製できなかった中大動物（ウサギ，ブタ，ウシ，サルなど）にも利用することが可能である。このようにZFN技術は従来のES細胞技術に比べて様々な利点があることから，新しい遺伝子改変技術として注目されている。

Ⅱ．重症複合免疫不全（SCID）[用語3]ラット

われわれは，このZFN技術により，X連鎖重症複合免疫不全（X-SCID）の原因遺伝子を破壊した*Il2rg*ノックアウトラットを作製した（図❸A）[5]。ZFN技術により作製されたX-SCIDラットは，野生型と同様に発育したが，剖検してみると胸腺が著しく萎縮していた。血漿IgGは半減し，血漿IgAはほとんど検出できなかった。フローサイトメトリー解析の結果，X-SCIDラットの末梢血では，$CD4^+CD8^-$T細胞が減少しており，$CD4^-CD8^+$T細胞はほとんど存在しなかった。末梢血中には，成熟B細胞およびNK細胞もほとんど存在しなか

図❸　X-SCID ラット（*Il2rg* ノックアウトラット）の免疫不全症

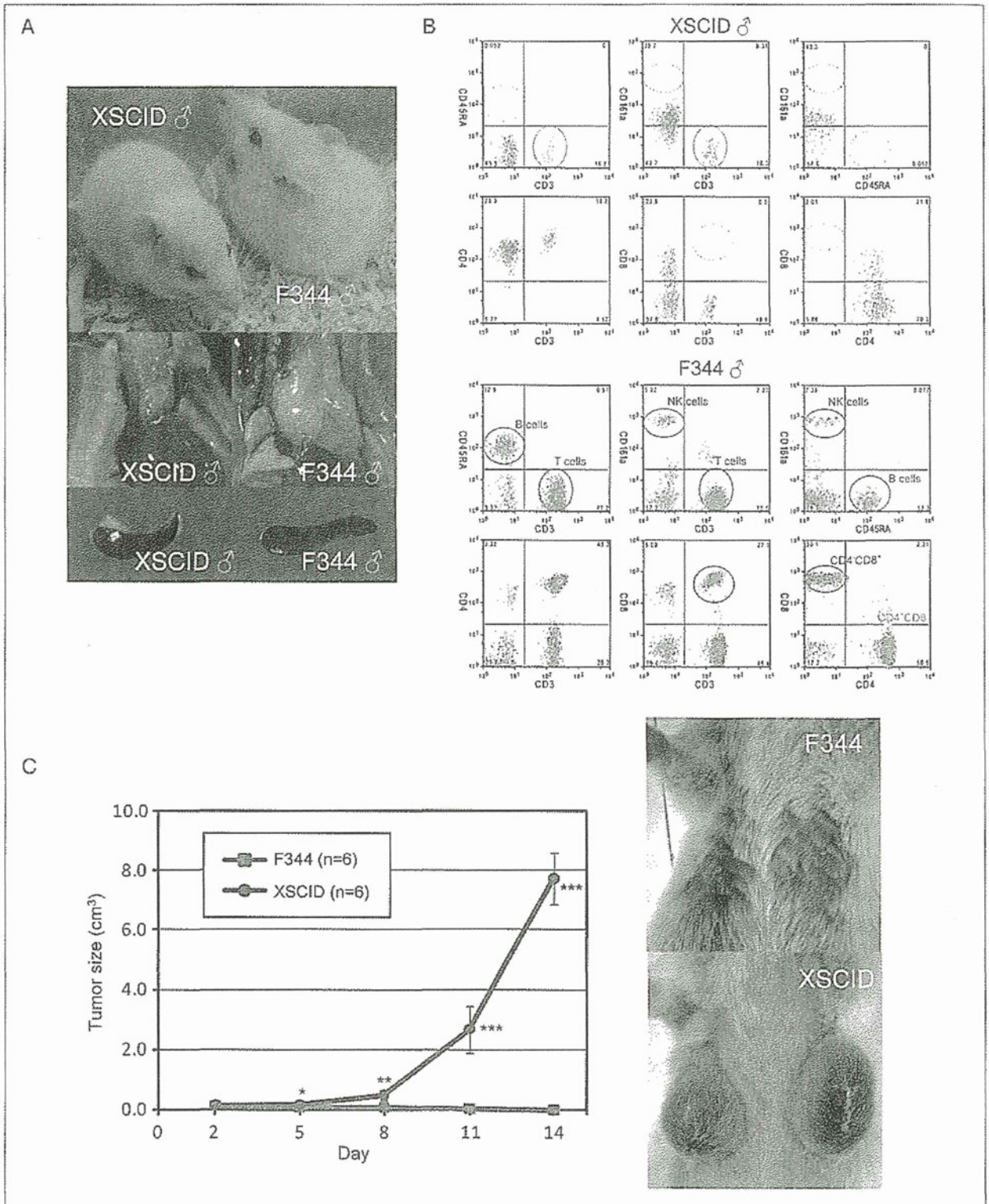

A.　作製された X-SCID ラットは，正常とほぼ同様に成育したが，胸腺皮質が著しく萎縮していた。
B.　フローサイトメトリー解析の結果。X-SCID ラットの末梢血には T 細胞が顕著に減少しており，B 細胞および NK 細胞はほとんど存在していなかった。
C.　ヒト卵巣がん細胞株を X-SCID ラットの皮下に移植することで，ヒト卵巣腫瘍をラット体内に作製することができる。
（グラビア頁参照）

った（図❸B）。ヒト卵巣がん細胞株の皮下移植による担がん試験を実施した結果，対照のF344ラットでは，ヒト卵巣腫瘍細胞の増殖を抑制したのに対し，X-SCIDラットはすべての個体で腫瘍細胞が増殖した（図❸C）。SCIDマウスは，ヒト細胞や組織の移植研究，移植したヒト細胞に対する薬理試験あるいは毒性試験などに多用されている。X-SCIDラットは，がん研究，幹細胞移植研究，創薬研究などに幅広く利用されるモデル動物になるであろう。

マウスでは，*Il2rg*遺伝子をノックアウトしたX-SCIDマウスより，*Prkdc*遺伝子を欠損したSCIDマウスが広く利用されている。さらにはⅠ型糖尿病モデルNODマウスに*Prkdc*遺伝子を欠損させたNOD-*scid*や，NOD背景系統に*Prkdc*遺伝子と*Il2rg*遺伝子両方を欠損させることで，T細胞，B細胞，NK細胞すべてを欠失したより重症の免疫不全動物NOGマウスが開発されている[8]。筆者らはZFN技術を利用して*Prkdc*遺伝子を欠損したSCIDラット，*Prkdc*遺伝子と*Il2rg*遺伝子両方を同時に欠損したFSG（F344-*scid Il2rg*）ラットを作製することに成功した（投稿中）。SCIDラットは，マウスと同様に胸腺の委縮，T細胞，B細胞の欠失が認められた（図❹A）。SCIDマウスでは，一部の個体あるいは加齢とともに血中IgGなどの免疫グロブリンが検出される‘Leaky’と呼ばれる現象が認

図❹ SCIDラット（*Prkdc*ノックアウトラット）

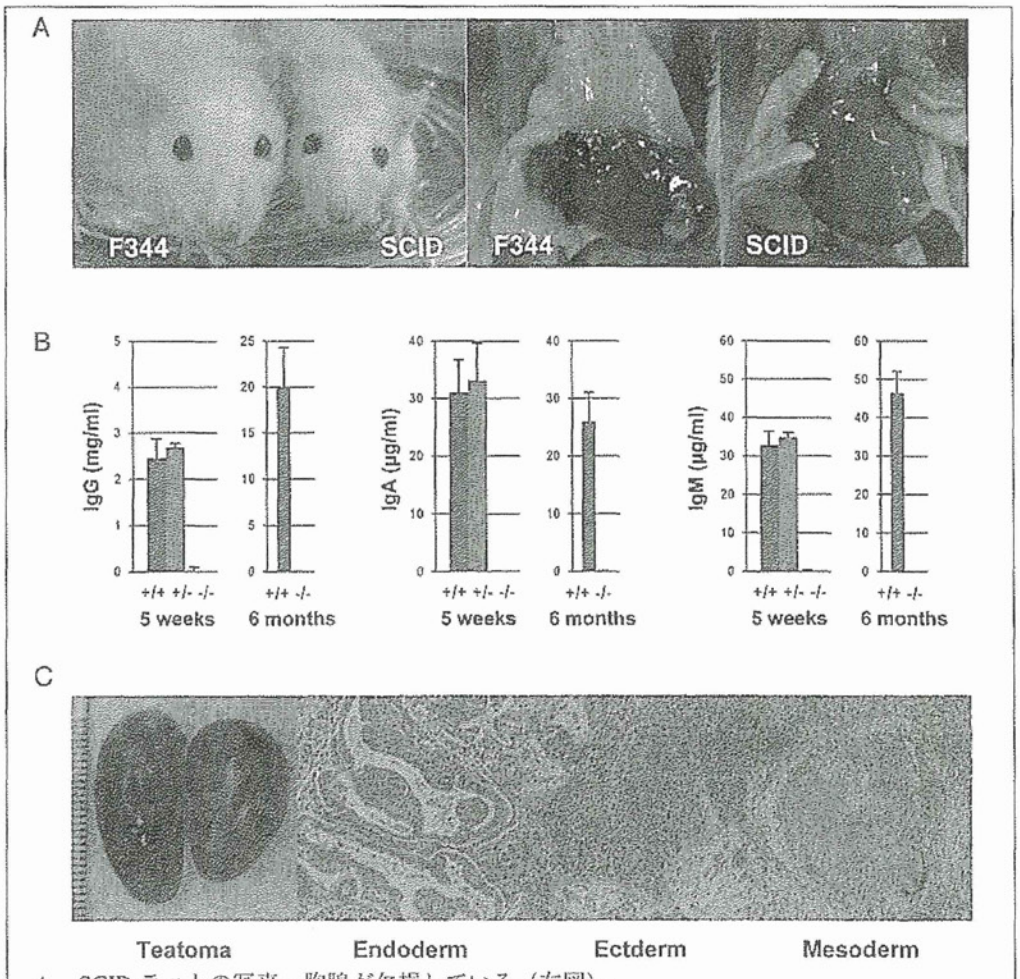

A. SCIDラットの写真。胸腺が欠損している（右図）。
B. 免疫グロブリン（IgG，IgA，IgM）を血液中に産生することができない。
C. ヒトiPS細胞をSCIDラットの精巣に移植することで，内胚葉，中胚葉，外胚葉由来の多種類の分化した細胞を含んだテラトーマ（奇形腫）を形成した。 （グラビア頁参照）